

Design and development of steering and suspension system of a concept car

SAMUEL JOSEPH



**KTH Industrial Engineering
and Management**

Master of Science Thesis
Stockholm, Sweden 2013

Design and development of steering and suspension system of a concept car

Samuel Joseph



Master of Science Thesis MMK 2013:23 MKN077
KTH Industrial Engineering and Management
Machine Design
SE-100 44 STOCKHOLM



KTH Industrial Engineering
and Management

Master of Science Thesis MMK 2013:23 MKN077

Design and development of steering and suspension system of a concept car

Samuel Joseph

Approved 2013-06-05	Examiner Ulf L Sellgren	Supervisor Kjell Andersson
	Commissioner KTH Transport Demo Lab	Contact person Peter Georén

Abstract

Today, the primary goal of every automotive industry is to improve the fuel efficiency, which leads to a focus on developing lighter vehicles, compact cars, with a minimum of rolling-resistance. As a consequence of this, we need to put more attention to the stability of the vehicle when manoeuvring in turns and at evasive actions.

The design of the steering system plays a vital role in stability and control of an automobile. There are three main parameters to be optimized for this regard, namely camber, caster and toe angles. Among these three, the camber angle plays a predominant role in vehicle control. If a car has a high negative camber angle, it is more stable. But high camber angle values are required only in some extreme cases like high speeds or emergency manoeuvring. However, a high negative camber angle also has a negative effect on the fuel efficiency of the vehicle.

Instead of having fixed values an active control of camber angle is preferred which results in very good control of the vehicle without affecting the fuel efficiency. Thereby, the camber angle can be varied based on the vehicle's response and drive pattern of driver. Much work has been made in this area, resulting in many conceptual design solutions. This project deals with a new concept where a variable camber can be obtained by active control.



KTH Industrial Engineering
and Management

Examensarbete MMK 2013:23 MKN077

Design och utveckling av styr-och fjädringssystem för en konceptbil

Samuel Joseph

Approved 2013-06-05	Examinator Ulf L Sellgren	Handledare Kjell Andersson
	Uppdragsgivare KTH Transport Demo Lab	Kontaktperson Peter Georén

Sammanfattning

Idag är det främsta målet för varje biltillverkare att förbättra bränsleeffektiviteten vilket leder till att utvecklingen fokuseras mot att konstruera kompakta, mindre lättare fordon med lågt rull- och luftmotstånd. Detta medför även en ökad fokusering på fordonets stabilitet vid undanmanövrar och kurvtagning.

Utformningen av storsystemet spelar en viktig roll för stabiliteten och kontrollen av en bil. Det finns tre huvudsakliga parametrar som skall optimeras för detta hänseende, dvs hjulvinklarna för camber, caster och toe. Bland dessa tre, har camber en dominerande roll i kontrollen över fordonet. Om en bil har en stor negativ cambervinkel, är den mer stabil. Men höga värden på cambervinkel krävs endast i vissa extrema fall som vid höga hastigheter eller vid undanmanövrar. Däremot har en hög negativ cambervinkel en negativ påverkan av fordonets bränsleeffektivitet.

Istället för att ha fasta värden är aktiv reglering av camber att föredra, då det leder till mycket god kontroll över fordonet. Därigenom kan cambervinkeln varieras utifrån bilens respons och körmonster beroende på förare. Många undersökningar har gjorts på detta område och många koncept har utvecklats. Detta projekt handlar om ett nytt koncept där en variabel cambervinkel erhålls genom aktiv reglering.

FOREWORD

I would like to thank all those who have contributed with their help, guidance, motivation and assistance during my thesis work.

This master thesis work was done in KTH- Transport lab as a concept vehicle design. First of all, I would like to express my deepest sense of gratitude and thank to my supervisor and teacher Professor Kjell Andersson at the KTH, Machine Design, who offered his continuous advice and encouragement throughout the course of this thesis. I thank him for the systematic guidance and great effort he put into training me in the scientific field.

I thank Peter Georén, the Project Manager KTH Transport Labs, for supporting my decisions and, Associate Professor Lars Drugge, Vehicle dynamics division, for his comments and suggestion in lighting up the start of my thesis. I would like to immensely thank Thomas Östberg, Lab and Workshop supervisor, for manufacturing number of components. In spite of the language barrier, his patience and suggestions in modification ignited new ideas in me for this thesis.

I also thank Mikael Nybacka, Assistant Professor of Aeronautical and vehicle engineering, who helped me so much in assisting with the Adams car software, for extracting results from it.

I thank my parents, siblings for their trust they had in me, by supporting me mentally and financially throughout my Master's degree. I also thank all my friends across the world, who gave me motivation to reach this place till today.

Last but certainly not the least, I thank god almighty for the wisdom and perseverance that he has been bestowed upon me during this research project, and indeed, throughout my life: “என்னைப் பெலப்படுத்துகிற கிறிஸ்துவினாலே எல்லாவற்றையுஞ்செய்ய எனக்குப் பெலனுண்டு”. (Philippians 4: 13)

Samuel Joseph

Stockholm, May 2013

NOMENCLATURE

Here are the notations and abbreviations used in this thesis.

Notations

Symbol	Description
E	Young's modulus (Pa)
a_v	Acceleration of the vehicle
R	Turing radius of car
M	Total mass of the car
v	Speed of the vehicle
rpm	Rotations Per Minute
M_N	Motor torque
F_x	Force on longitudinal direction
F_y	Force on vertical direction
F_z	Force on Lateral direction
FOS	Factor of Safety

Abbreviations

CAD	Computer Aided Design
ABS	Anti-lock Braking System
MR	Magneto Rheologic fluid
FEA	Finite Element Analysis
RCV	Research concept vehicle
UCA	Upper control arm
LCA	Lower control Arm

TABLE OF CONTENTS

ABSTRACT.....	iii
FOREWORD.....	vii
NOMENCLATURE.....	ix
TABLE OF CONTENTS.....	xi
LIST OF FIGURES	xv
LIST OF TABLES	xvii
1 INTRODUCTION.....	1
1.1 Background.....	1
1.2 Purpose.....	1
1.3 Scope.....	1
1.4 Delimitations.....	2
1.5 Method.....	2
2 FRAME OF REFERENCE.....	3
2.1 Steering system.....	3
2.1.1 Camber angle.....	3
2.1.2 Caster angle.....	4
2.1.3 Toe angle.....	4
2.2 State of the art.....	5
2.3 Suspension system.....	6

3 CONCEPTUAL DESIGN.....	9
3.1. Requirements specification.....	9
3.2 Concept generation.....	9
3.2.1 Concept 1 – Modified e-corner.....	9
3.2.2 Concept 2 – Worm wheel.....	10
3.2.3 Concept 3 – Jack link.....	11
3.2.4 Concept 4 – V-link.....	12
3.2.5 Concept selection.....	13
3.3 System kinematics.....	14
3.4.1 Adams analysis.....	17
3.4.2 Force selection.....	20
3.4.3 Adams result summary.....	21
3.5 Force calculation.....	22
3.5.1 Factor of safety.....	22
4 DETAIL DESIGN.....	25
4.1 Hub motor.....	26
4.2 A-Arm.....	27
4.3 Coupling hub.....	28
4.4 Steering column.....	29
4.5 Top bracket.....	31
4.6 Top pivot.....	32
4.7 V– Link.....	33
4.8 Bottom bracket.....	34
4.9 Range verification of camber angle.....	35

5 DISCUSSION AND CONCLUSIONS.....	37
5.1 Discussion.....	37
5.2 Conclusions.....	37
6 RECOMMENDATIONS AND FUTURE WORK.....	39
6.1 Recommendations.....	39
6.2 Future work.....	39
7 REFERENCES.....	41
APPENDIX.....	43

LIST OF FIGURES

The figures presented in this master thesis are listed in this chapter.

- Figure 2.1 Camber angle
- Figure 2.2 Caster angel
- Figure 2.3 Toe angle
- Figure 2.4 Rack and pinion steering
- Figure 2.5 Pitman arm steering
- Figure 2.6 Power steering
- Figure 2.7 Suspension systems. (a) Double wishbone, (b) Macpherson
- Figure 3.1 Siemens VDO e-corner concept.
- Figure 3.2 Pivot wheel camber control
- Figure 3.3 Worm wheel camber control
- Figure 3.4 Jack type camber control
- Figure 3.5 Jack link of jack type camber concept
- Figure 3.6 V-link Camber control (a) schematic diagram of concept, (b) having positive camber (c) Having negative camber)
- Figure 3.7 Schematic diagram of steering system configuration.
- Figure 3.8 Steer column and V-link's horizontal movement
- Figure 3.9 CAD model, showing the setup of the steering design.
- Figure 3.10 Adams Modelling subsystem co-ordinates
- Figure 3.11 Adams car model
- Figure 3.12 Forces & torque of upper control arm (UCA) inner.
- Figure 3.13 Forces & torque of upper control arm (UCA or V-link) front.
- Figure 3.14 Forces & torque of upper control arm (UCA or V-link) rear.
- Figure 3.15 Illustration of forces acting in different points of the suspension based on the Adams simulation.
- Figure 3.16 Illustration of forces acting in different points of the suspension based on the Adams simulation (with FOS).
- Figure 4.1 Isometric view of steering system
- Figure 4.2 Motor speed torque characteristics.

- Figure 4.3 CAD model of A-Arm.
- Figure 4.4 ANSYS verification showing stress values.
- Figure 4.5 CAD Model of Coupling Hub
- Figure 4.6 ANSYS verification showing stress values.
- Figure 4.7 CAD Model of Steering column.
- Figure 4.8 ANSYS verification showing stress values.
- Figure 4.9 CAD Model of Top Bracket
- Figure 4.10 CAD Model of shaft mating with the Top Bracket
- Figure 4.11 CAD Model of Top Pivot
- Figure 4.12 ANSYS verification showing stress values.
- Figure 4.13 CAD Model of V- link
- Figure 4.14 ANSYS verification showing stress values.
- Figure 4.15 CAD Model of V- link
- Figure 4.16 ANSYS verification showing stress values.
- Figure 4.17 CAD model showing maximum positive camber angle.
- Figure 4.18 CAD model showing maximum negative camber angle

LIST OF TABLES

The tables presented in this master thesis are listed in this chapter.

Table 3.1 Advantages and disadvantages of concepts.

Table 3.2 Pugh matrix concept comparison

Table 3.3 Input parameters for ADAMS modelling

Table 3.4 Factors of safety recommendation based on their load conditions

Table 3.5 Actual force induced and designing force values considering FOS

Table 4.1 Details of selected motor (Heinzmann PRA - 230 48 V DC)

In this chapter brief introduction, problem description, purpose and delimitations are presented. The thesis overview is discussed in brief.

1.1 Background

Whenever we rate a car, we look into many factors like power, mileage, style, comfort etc. Among all these, the most important factor is its ride control. Yes, a car, without good ride control is extremely dangerous. The ride handling of any car depends on steering system, suspension system, braking system etc. Due to popularity of using light-weight materials in designing and manufacturing of a car to increase fuel efficiency and reduce exhaust emissions demands on ride control have been more critical. New systems with active electromechanical control of ride handling have been proposed lately, but to achieve full potential of these systems they require adjustable kinematics.

The Anti-lock Braking System (ABS) for an improved brake system and the use of Magneto-Rheologic Fluids (MR Fluids) in suspension systems are examples of such systems. In steering systems we want to vary geometry to gain a better handling of the car. Much research has been done and is still in progress in this field.

One of the main ideas behind this project was to develop a design concept with a variable camber angle that will improve manoeuvring in turns and give better comfort when encountering a bump or pot-hole.

1.2 Purpose

The control of today's car is getting very critical. Manoeuvring in sharp turns, irregular road pattern also affects the control of the car. This project deals with the design and development of a new steering system for an electric car. The idea of this steering system is to have a variable camber angle during driving. This car is run by four in-wheel motors, with active steering and camber angle control. By doing so, the driver gets steady driving control and also provides comfort to the passengers.

1.3 Scope

The overall aim of the project is to create a steering system that has an adjustable camber angle during the ride. It was initially planned to have worm-wheel drives for varying both steering and camber angles, but this was later changed to be used for only the steering system. The scope of this project are

- Active camber control, i.e. control camber by electric motor
- Motor operated steering system
- Suitable suspension system
- Design and strength verification of entire system

1.4 Delimitations

The main aim of this project is to have a working model of an Autonomous Corner Module, ACM steering system. However, there are some delimitations in this project as follows,

- Design optimization for better compactness and strength are not included.
- Size and geometric optimization are not included.
- Selection of standard parts such as, bearings, lead screw, worm gear set, control motors are not included.

1.5 Method

The very first step was to brainstorm different ideas for designing a system to control the camber. Many of those concepts were studied and one particular concept was selected based on its feasibility, rigidity and ease of manufacturing and operation.

From the selected concept, components were modelled for optimum functionality and strength and verified in ANSYS for final system.

2 FRAME OF REFERENCE

A study is performed on various parts of a steering and suspension system. Some of the popular steering systems are briefly discussed. Major parameters that influence a steering system are also discussed here.

2.1 Steering system

The main aim of steering is to guarantee that the wheels are pointing in the desired direction. The steering system of an automobile includes all parts right from driver's steering wheel to the tire. In a steering system, camber, caster and toe angles are the very crucial parameters that decide the functionality of the car's ride control.

2.1.1 Camber angle

Camber angle is the angle (in degrees), between the perpendicular from the ground and the centre line of the wheel, as seen from car's front. If a car is running in a straight line, the centre line of the wheel should be perpendicular to the road, assuming the road is perfectly flat. This provides complete contact of wheel width on the road. But if the car is taking a turn, it generates a centrifugal force which tilts the centre line of the wheel about the ground. Even in extreme cases it may topple the car. In order to have better contact patch on the road and for the stability of the car, this angle is provided. As seen from the front of the car, if the centre line is inclined inwards, it is called negative camber, and if it is inclined outwards, it is called positive camber.

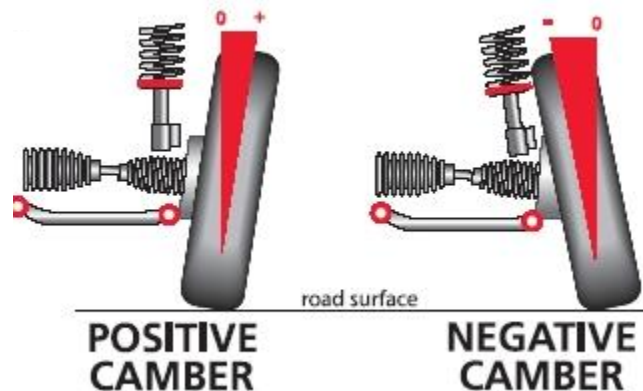


Figure 2.1, Camber angle [1]

By providing a camber, it also gains camber while cornering. This is a favourable condition because the outside wheel gains negative camber, while the inside wheel gains positive camber.

2.1.2 Caster angle

The caster angle is the angle of inclination of steering pivot axis to the vertical line from ground when viewed from side. This angle is provided to give vehicle's straight-line stability. While saying about caster angle, another parameter that comes along is trail. It is the distance between the steering axis and the wheel-to-ground contact patch. This distance is proportional to the force that causes the wheel to follow the steering.

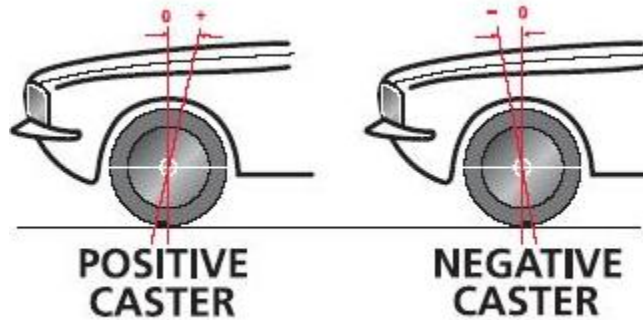


Figure 2.2, Caster angle [2]

2.1.3 Toe angle

Toe can be described in two ways. The toe angle is the angle to which the wheels are out of parallel, or angle of wheel centreline along the length of the vehicle. Toe can also be described as the difference between the track widths as measured at the leading and trailing edges of the tires. If there is any small disturbance in the road, the wheel will steer towards Toe settings affect three major areas of performance: tire wear, straight-line stability and corner entry handling characteristics.

If one side wheel of the car encounters a disturbance, that wheel is pulled back about its steering axis. By providing toe-in, the wheels are to tend to roll along paths that intersect each other. This provides directional stability. On contrary, by giving toe-out, the car always tries to take a turn. However, higher values of toe-in results in tire wear.

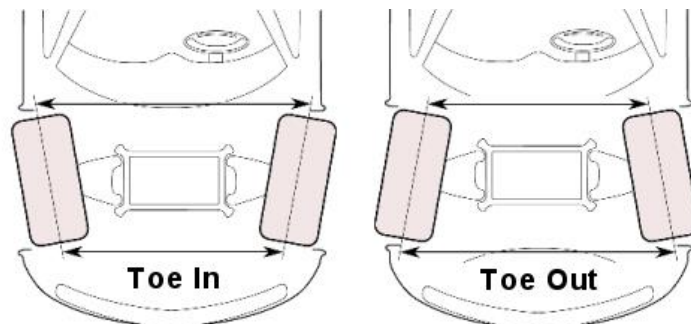


Figure 2.3 Toe angles [3]

In this project, since the steering system is controlled by motors, the stability is greatly controlled even without any caster and toe-in.

2.2 State of the art

The objective of steering system is to make the car to follow a desired direction. The conventional steering system includes a steering wheel, the steer column with universal joints, rack and pinion arrangement, which then is connected to stub axle through a link with a ball joint.

The rack and pinion design has the advantages of a large degree of feedback and direct steering "feel". A disadvantage is that it is not adjustable, so that when it does wear and develop lash, the only cure is replacement.

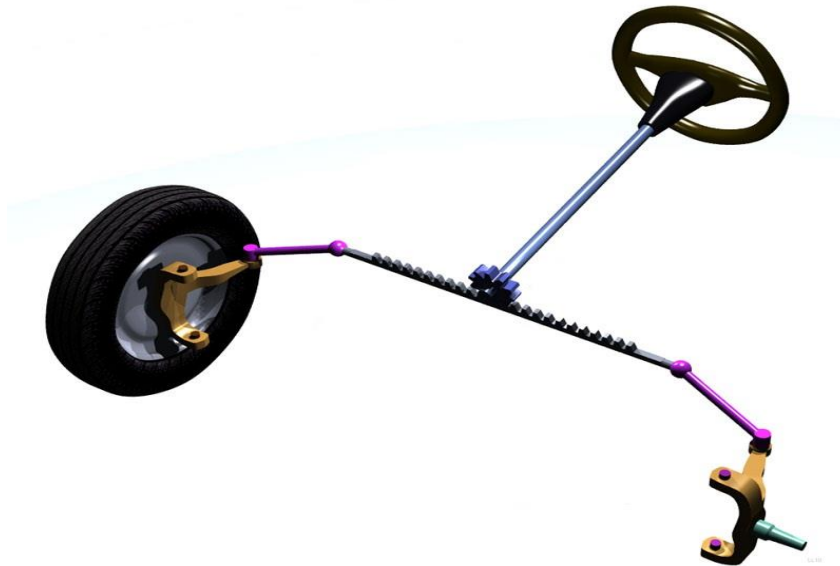


Figure 2.4 Rack and pinion steering [4]

The Pitman arm (worm and sector gear) was introduced to handle tough loads as like in trucks. This is added with recirculating balls between the teeth of the worm to reduce the friction.

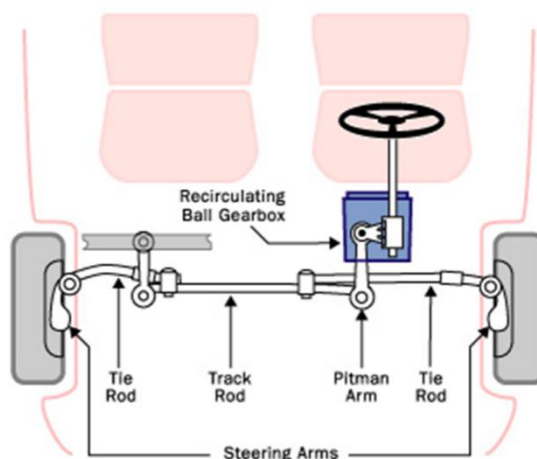


Figure 2.5, Pitman arm steering [5]

The steering effort is more when the car is moving in slow speed or not moving at all. Here rack and pinion arrangement is replaced with Hydraulic power steering (HPS) which can ease the steering operation. On further energy saving, the same rack and pinion is replaced with Electric power steering (EPS). There are also speed sensitive steering, all wheel steering. In active four wheel steering, we can have high stability and very small turning radius too.

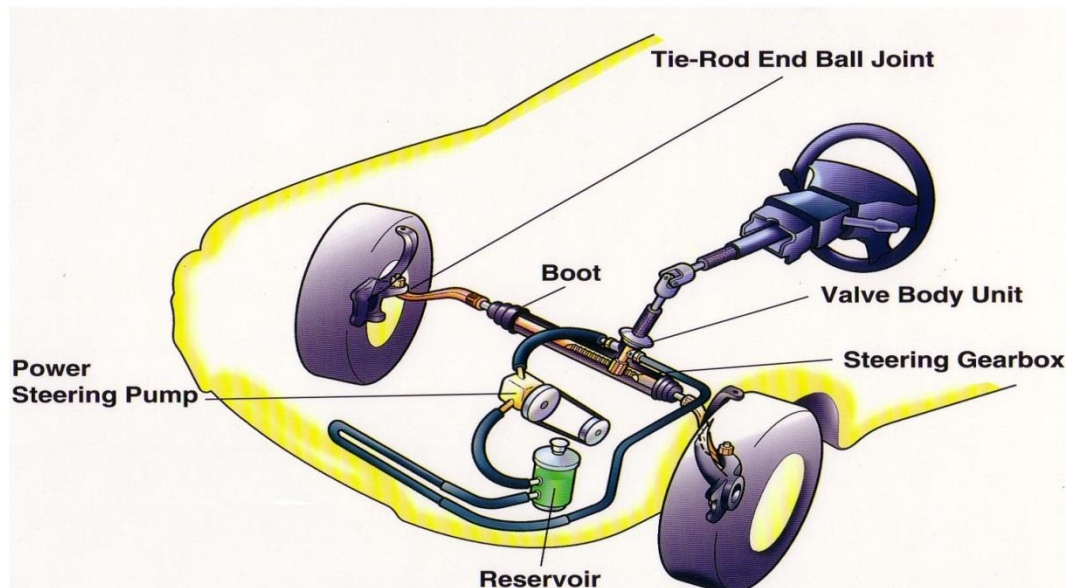


Figure 2.6, Power steering [6]

The concept car of this thesis has active steering system and can also have independent steering angle, thereby pirouette can be done when the car is stopped.

2.3 Suspension system

There are two important functions for a suspension system. The first function is to isolate the car from road shocks and vibrations. If this is not done, it may cause discomfort to the passengers or even damage to the goods inside.

Its second function is to ensure the wheel is always in contact with road irrespective of road surface. This gives the car maximum thrust in driving, grip in braking and control during manoeuvring.

As a steering system, there are two types namely, independent suspension and solid axle. However, most of the modern cars use only independent suspension system. The suspension action is accomplished with help of springs and dampers. Dampers are used to control spring action. There are leaf springs, coil springs, torsion springs, air suspension etc., to provide the necessary suspension. The type of spring is selected based on required comfort, load capacity, room space availability and cost. There are also hydraulic, Magneto Rheological (MR) fluid suspension, and electronic suspension for ultimate comfort and control.

There two famous suspension arrangement that most cars use, namely Macpherson strut and double wishbone.

In double wishbone structure, there are two arms (A) connected to the stub axle, and suspension is connected to the body from the lower arm. In Macpherson strut, lower end of stub axle is connected to the body through a rigid link and the top end connects to the suspension. This strut itself bears the load. The former one has a parallelogram system that allows the spindles / tyre to travel vertically up and down. However the later one holds good for front wheel drive cars, since there is ease of power transmission from gearbox.

The suspension used in this project is a normal coil-over type suspension that is found in most of the cars today. And it has a little modified version of conventional wishbone structure to incorporate the variable camber control.

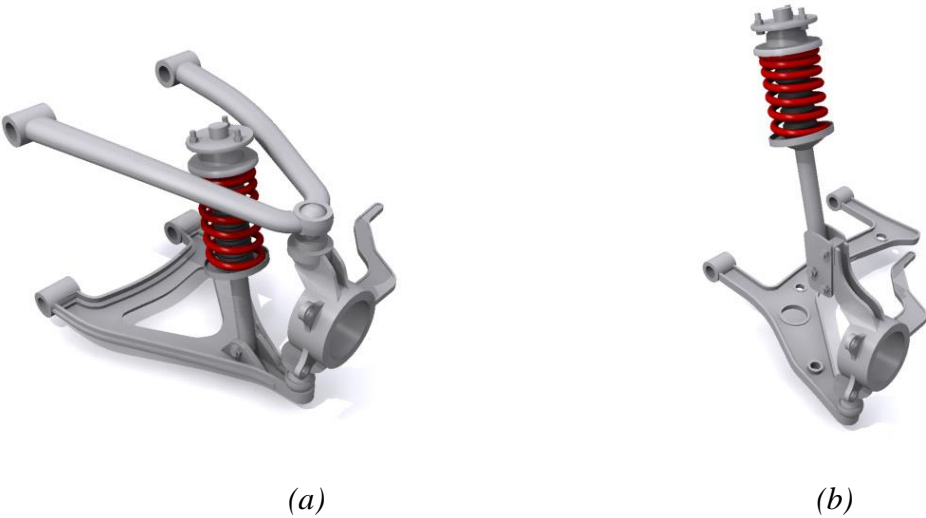


Figure 2.7, Suspension system (a) Double wishbone, (b) Macpherson [7]

3 CONCEPTUAL DESIGN

This chapter explains in detail the working procedure adopted for this thesis. Developments of mechanical structure from brainstorming ideas are briefly discussed. Some requirement specifications and assumptions made for desired functions are discussed. ADAMS modelling and result extractions, and follow up by CAD and ANSYS are also discussed here.

3.1. Requirements specification

- Track width : 1400 mm
- Wheel base : 2000 mm
- Weight M : 500 kg (including passengers)
- People : 2 (Side-by-side)
- Engine : in-wheel electric motor (4)
- Max speed (v) : 90 km/h.
- Maximum acceleration (a_v) : $1.8 \text{ m/s}^2 \Rightarrow$ (0-80 km/h in 12.3 sec)
- Camber control range : -10° to $+5^\circ$ [originally $\pm 10^\circ$]
- Minimum turning radius R : 5000 mm
- Braking distance : 45 m @ 80 km/h.
- Suspension : Wheel total vertical movement 130 mm (minimum requirement)

3.2 Concept generation

3.2.1 Concept 1 – Modified e-corner

The first concept is based on Siemens VDO e-corner concept and is shown in figure 3.1.

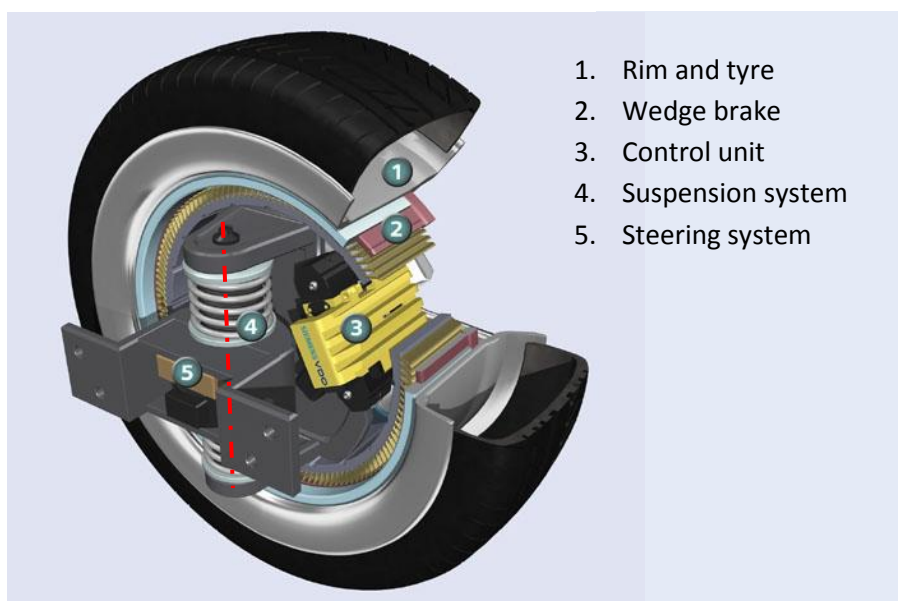


Figure 3.1, Siemens VDO e-corner concept [8]

In this e-corner concept, the car wheel can steer about the vertical axis (red line) shown in Figure 3.1. This same axis is the used as suspension axis for the car. There are two helical spring and damper units attached to the mount.

To the e-corner concept we have added a motor that can tilt the steer column and thereby provide a variable camber (Figure 3.2). However, using a single pivot concept becomes a crucial point in worst case which is undesirable. Moreover, its main strength is for large tyre vehicles that can incorporate in-wheel motors, enabling the steer axis to pass through the wheel-road contact point to get minimum wear.

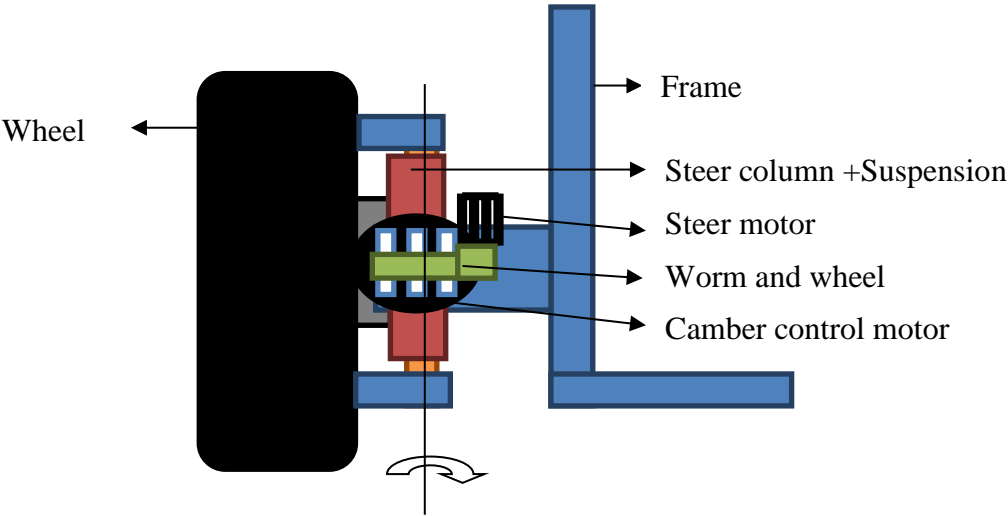


Figure 3.2, Pivot wheel camber control

3.2.2 Concept 2 – Worm wheel

The next concept shown in Figure 3.3 has solved the problem that it can be used for small wheel cars as well. However, the steering motors are adding unsprung mass which is undesirable for better suspension system. Another drawback is that the top worm and wheel mechanism is subjected to hold the weight of the car. In other words, some few teeth in worm wheel have to take a huge load.

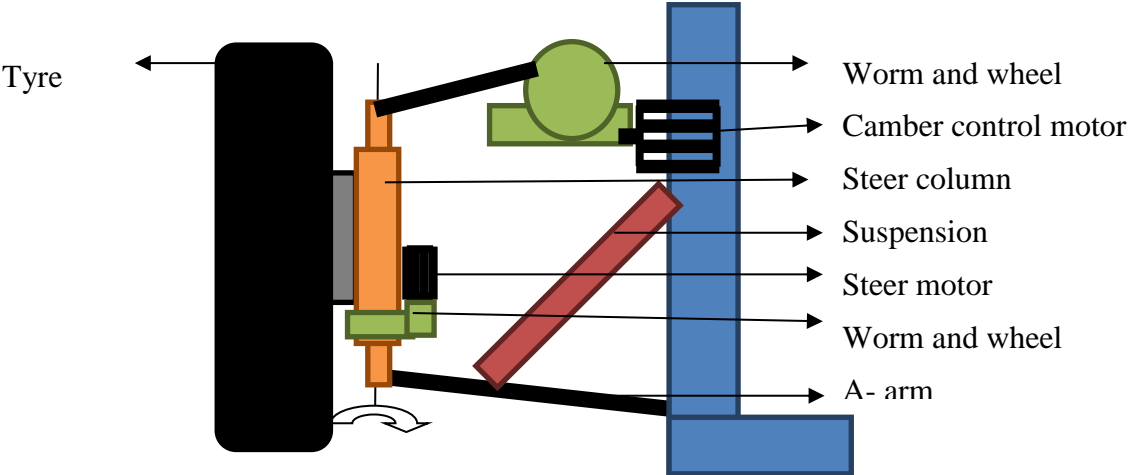


Figure 3.3, Worm wheel camber control

3.2.3 Concept 3 – Jack link

This concept (see Figure 3.4) overcomes the drawbacks with the previous concept. Here a jack like arrangement (Figure 3.5) is provided instead of a top link. This keeps the top link suitable for a more even load distribution. The drawbacks with this concept are that it is more complicated to manufacture and that it is adding unsprung mass to the suspension.

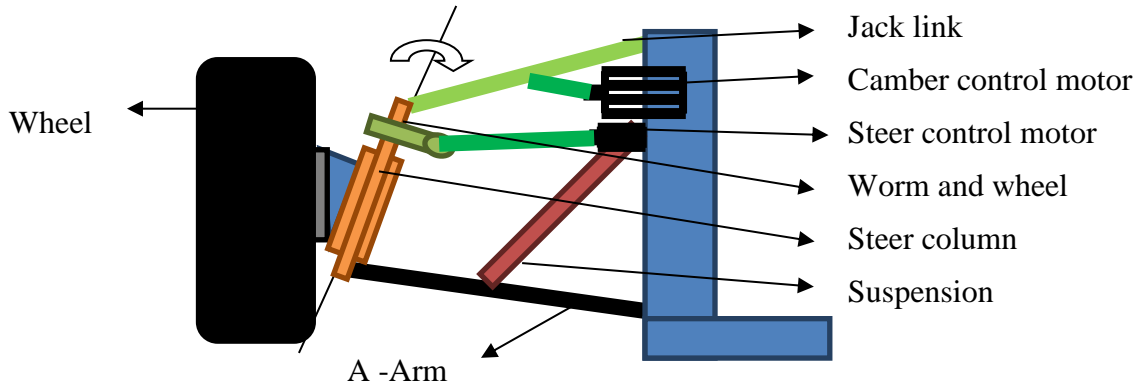


Figure 3.4, Jack type camber control

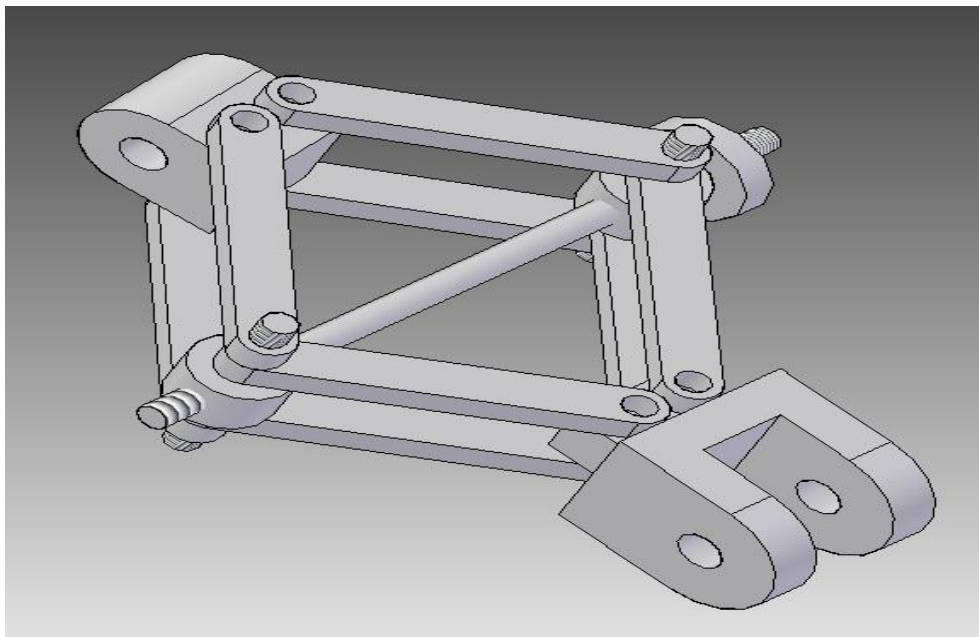


Figure 3.5, Jack link of jack type camber concept

3.2.4 Concept 4 – V-link

On further brainstorming, the Jack link is further optimized to minimize size and reduce unsprung mass. Two slider blocks are allowed to move along the sides and the links connected to this make the wheel have the variable camber.

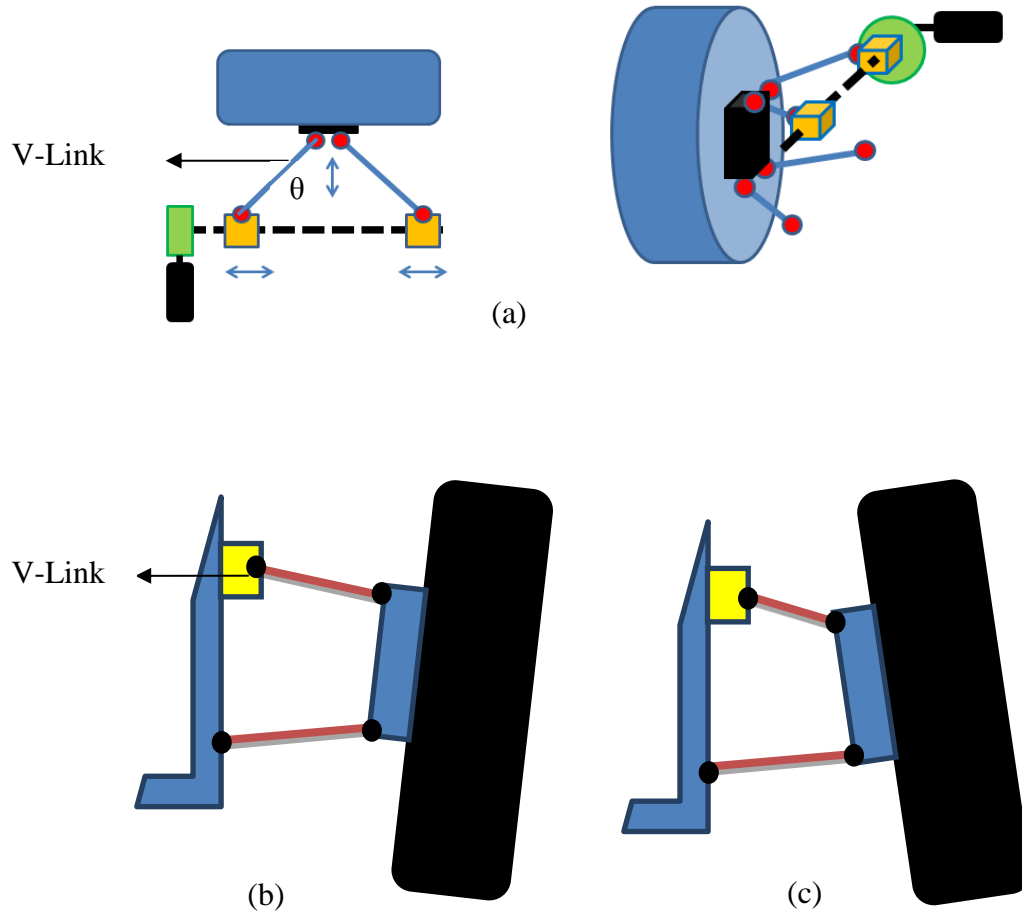


Figure 3.6, V-link Camber control (a) schematic diagram of concept, (b) having positive camber
(c) Having negative camber

It can be seen that, by reducing angle made by V-link, the camber angle is increased. Also happens in vice versa.

3.2.5 Concept selection

An evaluation of the generated solution concepts is made in two different ways. Firstly a list of advantages and disadvantages is made for each concept (Table 3.1). Secondly, Pugh's method for concept evaluation [23] is applied, see Table 3.2.

Table 3.1 Advantages and disadvantages of concepts.

Concept	Advantages	Disadvantages
Modified e-corner	Compact	Larger tyre and rim is needed to accommodate all system parts.
Worm wheel	Simple system	Complete load of car acts just on few teeth on worm wheel, which is risky.
Jack-link	Optimum space occupied and minimum wear in tyre	Jack mechanism, by itself is little complex.
V-link	Reliable, low unsprung mass	Lead screw with both right and left hand thread is critical to manufacture.

Table 3.2 Pugh matrix concept comparison [23]

Criteria	Concept			
	1 - Mod. e-corner(Ref)	2 - Worm wheel	3 - Jack link	4 - V-link
Camber $\pm 10^\circ$	S	S	S	S
Suspension adaptability	S	+	+	++
Adaptability with selected motor	S	+	+	+
Accessibility	S	+	S	++
Manufacturability	S	++	S	+
Minimum tyre wear	S	+	+	+
Robustness	S	S	++	+
Minimum unsprung mass	S	S	S	+
Score	0	+6	+5	+9
Sum of +ve $\sum +$	0	6	5	0
Sum of -ve $\sum -$	0	0	0	0
Sum of same $\sum s$	8	3	4	1

From the above tables, we can conclude that the V-link concept (concept 4) has some advantages as compared to the rest of the concepts. Thus, this V-link concept is chosen for further design and development.

3.3 System kinematics

For the chosen concept to work as intended, having the desired camber angle range, the length of A-arm, V-link, steer column height were to be chosen. It is preferable to have system as compact as possible. The major impact on the size is given by the steer column. Thus, the steer column is modelled with the following parameter assumptions (see figure 3.7).

Diameter of motor shaft (motor rotor)		=35mm
Heinzmann PRA - 230 48 V DC [9] (D_s)		
Coupling outer diameter (D_c)		= 60mm
Minimum thickness of coupling hub (Assumption)		= 10 mm
== > Coupling hub outer diameter (D_h)		= 80mm (at least)
Worm & wheel system height for steering mechanism (H_w)		= 10 mm
Pivot extension at top and bottom of steer column (H_p) = 30 + 30		= 60 mm
Total length of steer column (H_T)	$\geq D_h + H_w + H_p$	=80 +10 +60
		= 150 mm

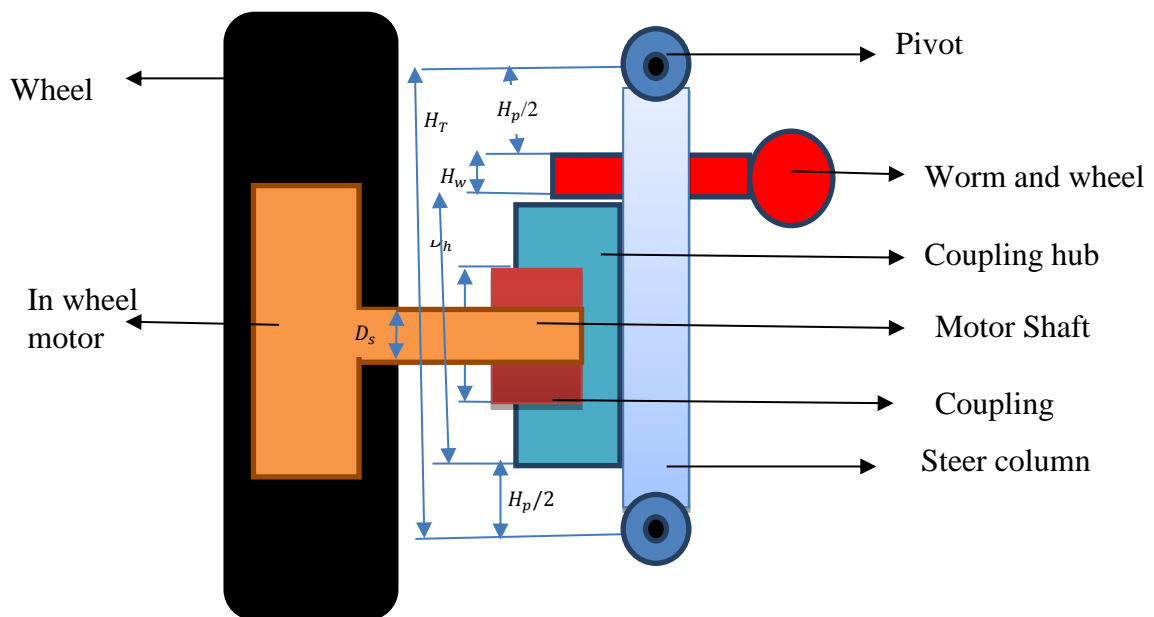


Figure 3.7 Schematic diagram of steering system configuration.

Thus, with the height of steer column, the required length of A- arm and V- link can be predicted.

For '0' camber angle, the length of A- arm will be equal to length of V-link. However, in normal wishbone steering structure, the top wishbone is shorter than bottom wishbone in order achieve more negative camber while taking a turn.

Another requirement is about the suspension and tyre deflection that influence the length required in both top and bottom links. If there is a need to have more up and down movement in tyre due to pit hole or a bump, which should not be reflected in chassis, the required length of A- arm and V-link increases.

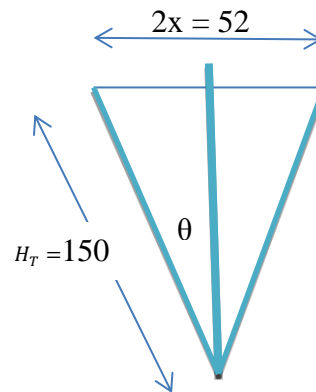


Figure 3.8 Steer column and V-link's horizontal movement

As we look, just into camber variation, and A- arm is horizontal, in order to have $\pm 10^\circ$, the shift of top pivot horizontally can be calculated.

$$x = 150 \sin \theta = 26$$

$$2x = 52 \text{ mm}$$

So V-links are pivoted at both the ends $\Rightarrow 20 + 20 = 40 \text{ mm}$

Thus, to have camber angle working in range of $\pm 10^\circ$, the V-link should be at least of length.

$$= 52 + 40 = 92 \text{ mm}$$

These two V-links are connected to sliders which move along the lead screw as shown in Figure 3.6 as yellow boxes. The minimum length of lead screw (and guide way) should be at least twice the length of V-link. Here, a guide way is introduced, so that the sliders will not rotate about the lead screw. In addition, the width of top pivot is also taken into account in deciding the length of lead screw. For this thesis, the design of lead screw from forces acting on it, were not calculated as mentioned before in the delimitations.

There are other mechanisms like hydraulic system, linear motor etc. that can replace this lead screw. But it is advisable to select a lead screw mechanism instead of linear motor or piston, so that it will have self-locking. However, advanced motors with self-locking capabilities can be deployed here if available.

If the wheel has landed on a bump of 65 mm, its steering column should shift up 65 mm, since it is connected rigidly to the wheel. Even at this situation, the system is expected to reach maximum negative camber (- 10°). So, to reach -10° camber the V-link length has to further decrease.

This exact value can be calculated, with trigonometric relations, provided the length of A- arm and steer column were properly defined. Since all three lengths are unknown, an iterative method of finding suitable minimum length is modelled in Solid Edge and it is animated to verify its range of operations.

Having the point of projection of steer axis, away from point of contact of road with tyre, will create wear in tyre, and also cause problems in sudden braking or quick acceleration. Thus it is decided to have an inclined steer column, so that, this projection point falls on the contact point, thereby achieving minimum wear. Thus the budding plane of coupling hub (surface that contacts to steer column) is inclined inward by an angle of 25°.

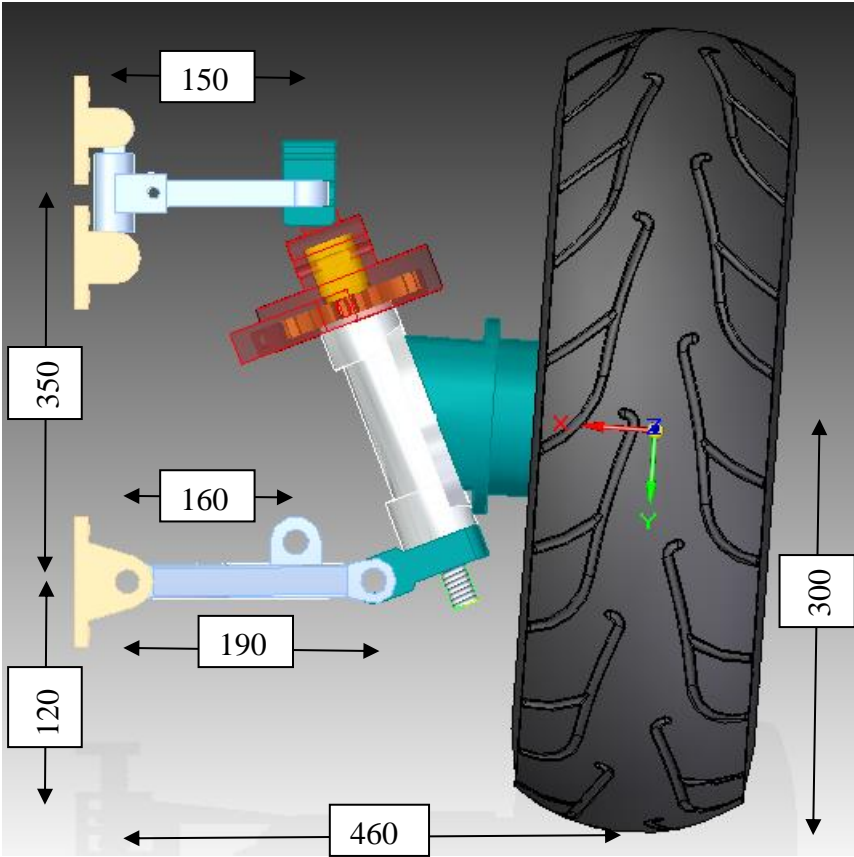


Figure 3.9 CAD model, showing the setup of the steering design.

The model is built with ideas of manufacturability in mind which are discussed in later chapters. The resulted model is shown below.

- A-arm length (between pivot points) = 190 mm
- Steer column (between pivot points, along with shaft) = 300 mm
- V-link (between pivot points) = 150 mm

3.4 Adams modelling

The V-Link camber control method was chosen due to its strength, stroke range and manufacturability. Adams Car was used for modelling and analysis of the concept as being part of the complete car. This was made in parallel with the development of the CAD model of the concept to include manufacturing considerations as much as possible.

The basis for the Adams model were the requirements specified in chapter 3.1.

3.4.1 Adams analysis

A model with defined geometry for kinematics is made in Adams-car. It is tested with three different scenarios.

1. Full braking

The car model is allowed to gain a speed of 90 km/h and then full braking is applied after 1 sec.

2. Taking a turn

The car model is subjected to take a turn of radius 5m. The forces induced due centrifugal action which reflects on the all pivot points in the system were noted.

3. Encountering a bump

The wheel of the car model is allowed to encounter a bump of 13 cm.

The input parameters for the Adams Car model is as follows,

Table 3.3 Input parameters for ADAMS modelling

Tyres	180/55R17 pac_mc_rear_tires.tir
Weight of tyre	20 kg
Tyre radius	320 mm
Velocity of vehicle	90 km/h
Turning radius	5000 mm
Bump height	130 mm
Track width	1400mm
Wheel base	2000mm

Since this thesis is about designing a new mechanical system, CAD modelling and ADAMS simulation were done in parallel. In other words, in design process, there were repeated looping cycles between CAD modelling and ADAMS simulations until a desired kinematics and no-interference CAD model was achieved. The subsystem parameters are shown in terms of geometric co-ordinates in figure 3.8.

The final input values which were derived from the CAD model were given as input measures in ADAMS to get the final model. The position co-ordinates of one of the four wheels in the Adams Car is shown below (see figure 3.9 for CAD model’s position dimensions).

	loc_x	loc_y	loc_z	remarks
hpl_drive_shaft_inr	0.0	-0.24	0.3	(none)
hpl_lca_front	-0.16	-0.24	0.12	(none)
hpl_lwr_strut_mount	0.0	-0.4	0.15	(none)
hpl_uca_front	-0.13	-0.24	0.47	(none)
hpl_top_mount	0.0	-0.24	0.35	(none)
hpl_wheel_center	0.0	-0.7	0.3	(none)

Figure 3.11, Adams modelling subsystem co-ordinates

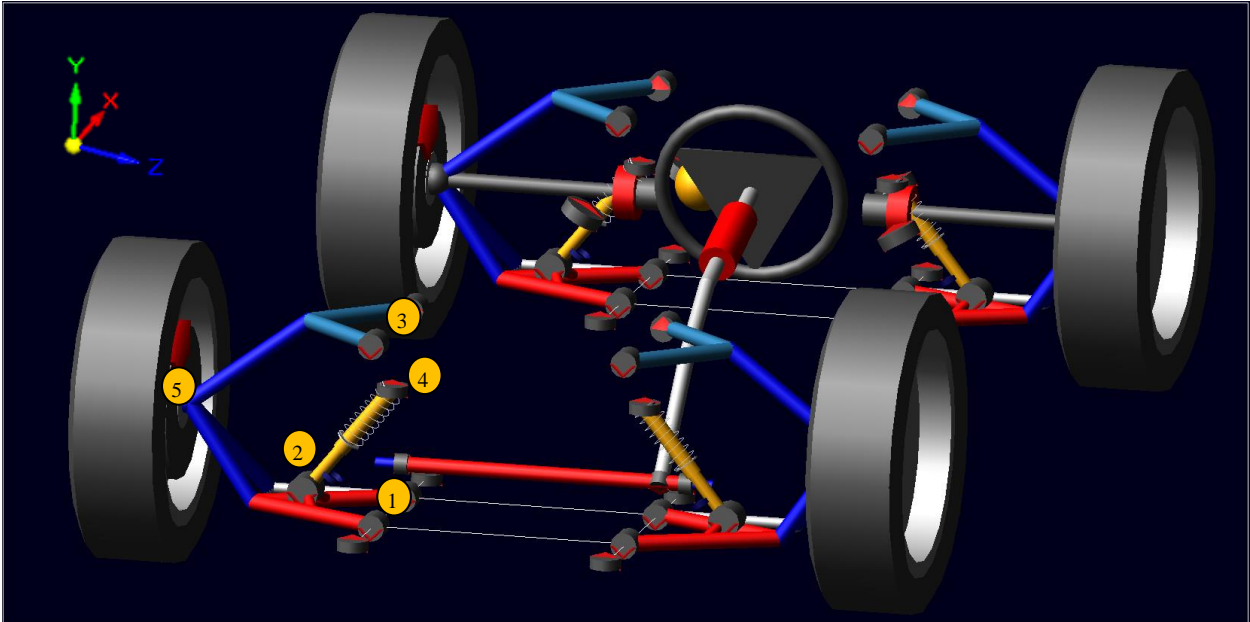


Figure 3.12 Adams Car model

From ADAMS, these plots were generated, and used in finding the maximum force induced in system at each point. These values are forces acting in x, y, z co-ordinates in respective points

For the first case, as the car is applied with full braking during a constant speed of 90 km/h and exerted forces in the critical points in the systems are plotted. Figure 3.13 shows the force values at the V-link inner end. Similarly, for every critical point, the force plots are generated. These values were accounted for ANSYS strength verification of the model. For force plots in other critical points, refer to Appendix.

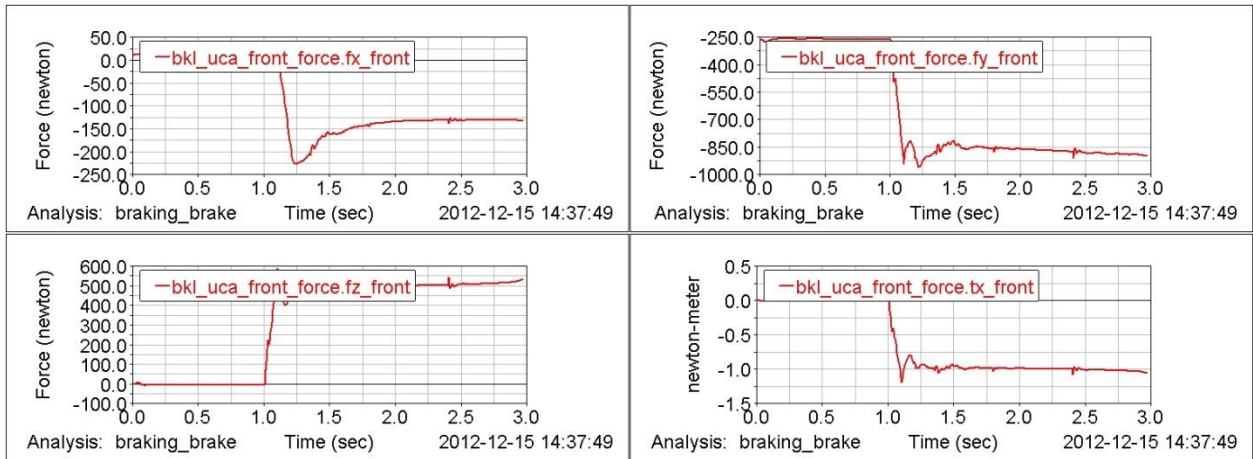


Figure 3.13 Forces & torque of upper control arm (UCA) inner.

For the second case, the car is subjected to take a turn of 5m and its forces at V-link inner are plotted and it's shown in Figure 3.14.

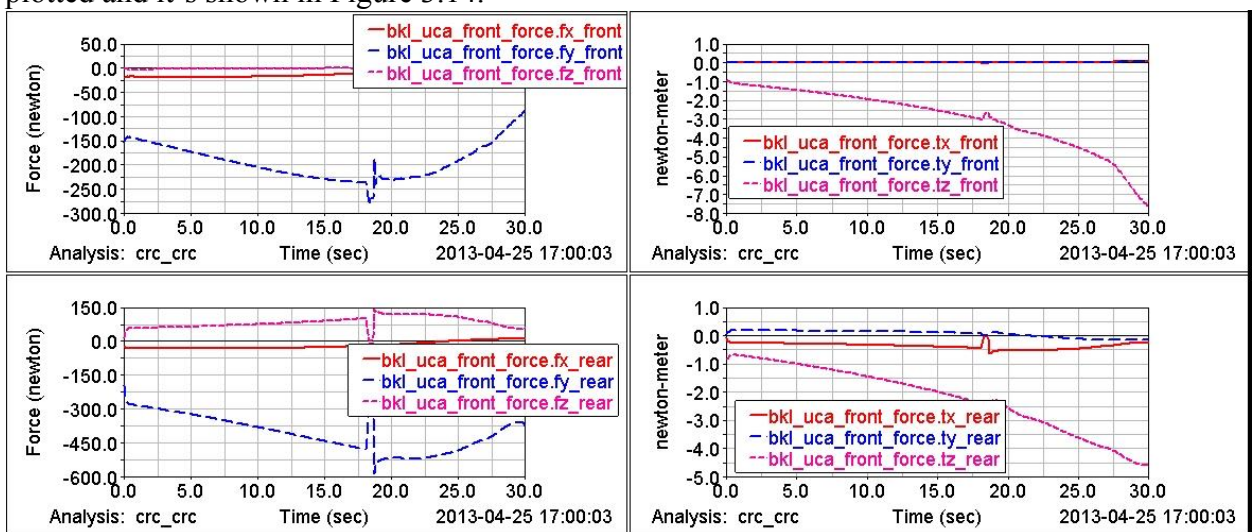


Figure 3.14 Forces & torque of upper control arm (UCA or V-link) front.

For the third case, the wheel of the car is subjected to encounter a bump of 13cm and its force values are plotted as shown below.

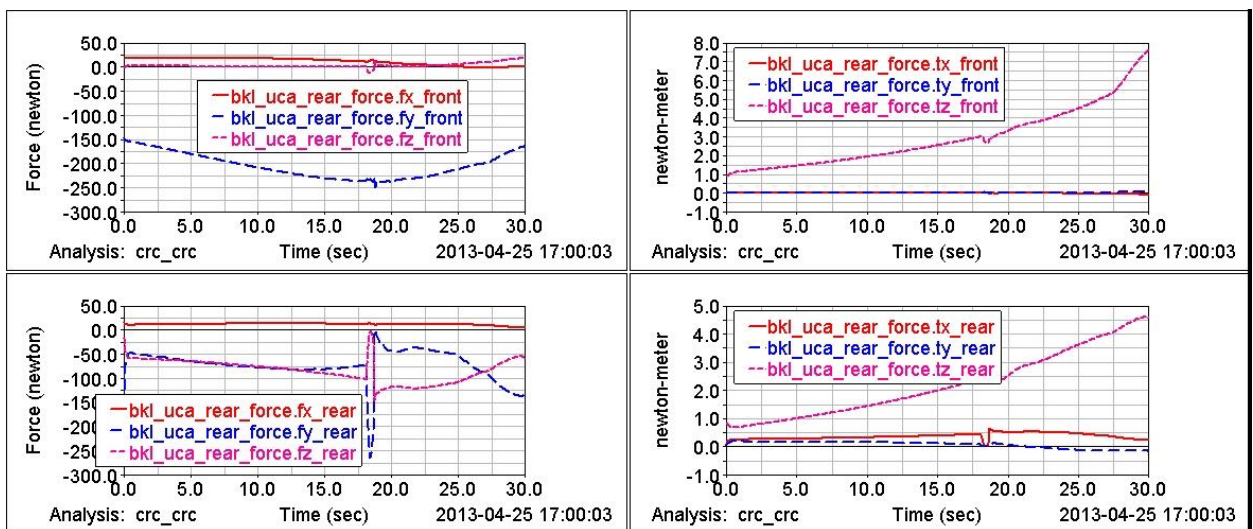


Figure 3.15 Forces & torque of upper control arm (UCA or V-link) rear.

With all these plots, forces at each connecting points are noted. These forces actually help in confirming the strength of Solid model with the help of ANSYS software.

3.4.2 Force selection

For the purpose of understanding of thesis document, just one of the pivot point (V-link inner) is discussed below.

From the plots shown in figure 3.13 referring to the first load case with full braking we found the maximum force values as;

$$\begin{aligned} F_x &= -230 \text{ N} \\ F_y &= -950 \text{ N} \\ F_z &= 550 \text{ N} \end{aligned}$$

Similarly, from the plots shown in figure 3.14 referring to the second load case with a radial turn we found the maximum force values as;

$$\begin{aligned} F_x &= 3 \text{ N} \\ F_y &= -22 \text{ N} \\ F_z &= 277 \text{ N} \end{aligned}$$

From the plots shown in figure 3.15 referring to the third load case of with a bump, we found the force values as;

$$\begin{aligned} F_x &= 20 \text{ N} \\ F_y &= -272 \text{ N} \\ F_z &= 147 \text{ N} \end{aligned}$$

From these three load cases we selected the maximum force in each direction as a basis for the design verification.

$$\begin{aligned} F_x &= -230 \text{ N} \\ F_y &= -950 \text{ N} \\ F_z &= 550 \text{ N} \end{aligned}$$

In the same way, the maximum forces acting in each pivoting points along corresponding coordinates were selected.

3.4.3 Adams result summary

From the plots in section 3.4.1 and the force selection method in section 3.4.2, the forces acting in each point have been visualized in figure 3.16. in the CAD model for easier understanding. Part models and its ANSYS verifications are discussed later chapter together.

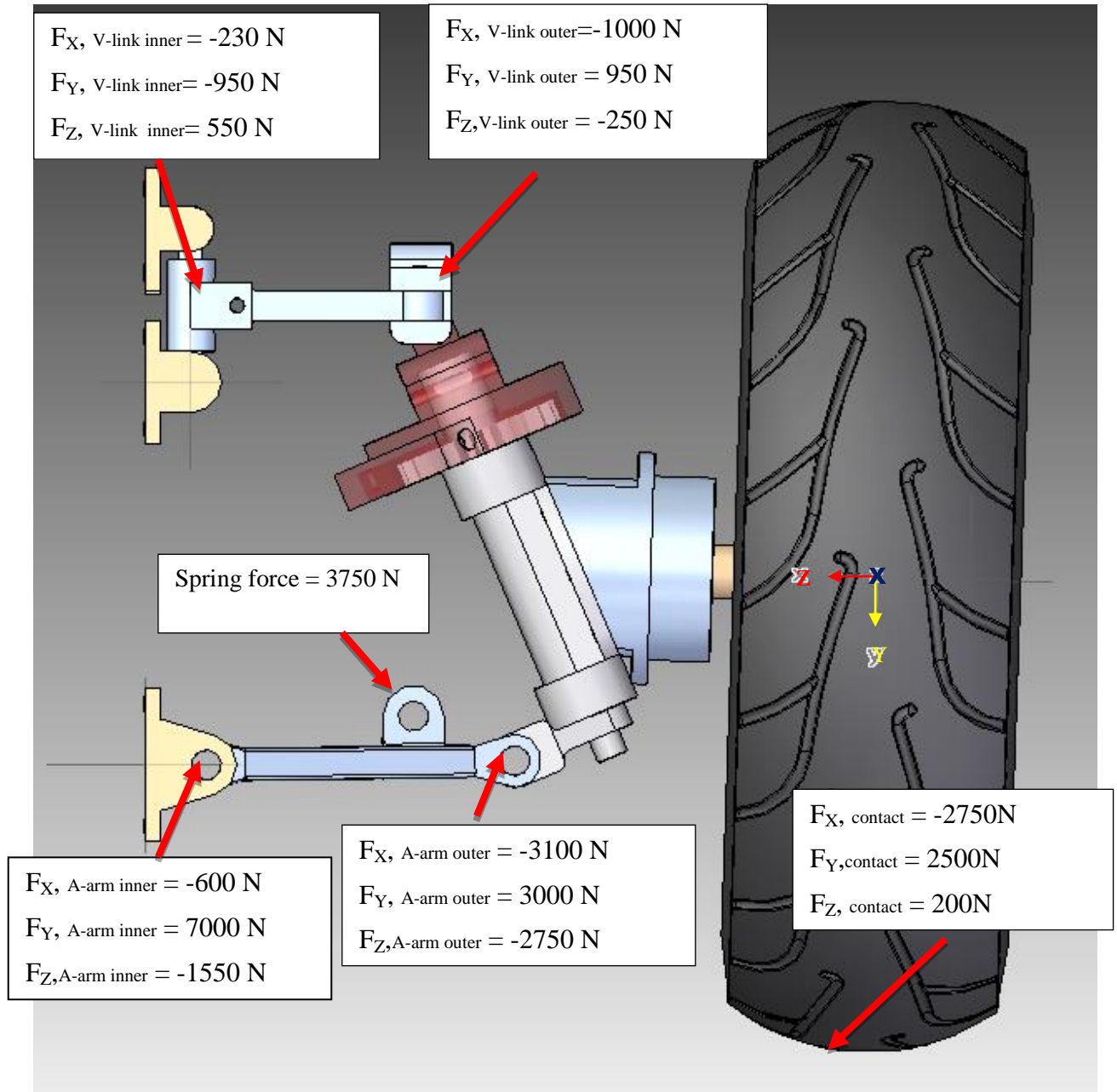


Figure 3.16 Illustration of forces acting in different points of the suspension based on the Adams simulation.

3.5 Force calculation

In any design, the part is always designed for the worst case. So that, the induced force will not cross the bearable limit of the part material.

3.5.1 Factor of safety

As we get into design any process, the term called Factor of safety (FOS) comes into picture. It is just the ratio of maximum bearable load to the maximum load applied. An optimum value of FOS should be chosen else, either performance or safety has to be compromised. It is always recommended to give safety value (>1) for a reliable working of the system/product. Factor of safety is also given because of imperfection in cast parts and various loading condition, and degree of safety required, as like in aircrafts, lifts, hoist, etc.

$$\text{Factor of safety (FOS)} = \frac{\text{Material strength}}{\text{Design load}}$$

The previous picture says just about the forces applied/induced in each point in the system. To add up factor of safety into account, these induced loads valued are multiplied by a safety factor, and that resulting values were used in ANSYS verifications.

Table 3.4 Factors of safety recommendation based on their load conditions [10]

Factor of Safety	Application
1.25 - 1.5	Material properties known in detail. Operating conditions known in detail. Loads and resultant stresses and strains known with high degree of certainty. Material test certificates, proof loading, regular inspection and maintenance. Low weight is important to design.
1.5 - 2	Known materials with certification under reasonably constant environmental conditions, subjected to loads and stresses that can be determined using qualified design procedures. Proof tests, regular inspection and maintenance required
2 - 2.5	Materials obtained from reputable suppliers to relevant standards operated in normal environments and subjected to loads and stresses that can be determined using checked calculations.
2.5 - 3	For less tried materials or for brittle materials under average conditions of environment, load and stress.
3 - 4	For untried materials used under average conditions of environment, load and stress.
3 - 4	Should also be used with better-known materials that are to be used in uncertain environments or subject to uncertain stresses.

Electric motor torque shaft : 1.1-1.2
 Axles and links, with repeated loading : 1.4-1.5
 Suspension : 2-2.5
 Lead screw, bidirectional load, fluctuating : 2-3

Hence after taking these values into account, the updated values are shown as follows

Table 3.5 Actual force induced and designing force values considering FOS

Force point		Maximum force induces	FOS	Resulting maximum forces
V-link, Fixed link end (inner)	F_x	-230	1.4	-322
	F_y	-950	1.4	-1330
	F_z	550	1.4	770
V-link, Movable link end (outer)	F_x	-1000	1.4	-1400
	F_y	950	1.4	1330
	F_z	-250	1.4	-350
Spring force (in designing spring)		3750	2.2	8250
Spring force (in designing A-arm)		3750	1.4	5250
A-arm, Fixed link end (inner)	F_x	-600	1.4	-840
	F_y	7000	1.4	9800
	F_z	-1550	1.4	-2170
A-arm, Movable link end (outer)	F_x	-3100	1.4	-4340
	F_y	3000	1.4	4200
	F_z	-2750	1.4	-3850
Tyre contact point	F_x	-2750	1.2	-3300
	F_y	2500	1.4	3500
	F_z	200	1.4	280

After taking factor of safety into account, the resulting loads are shown in Figure 3.17.

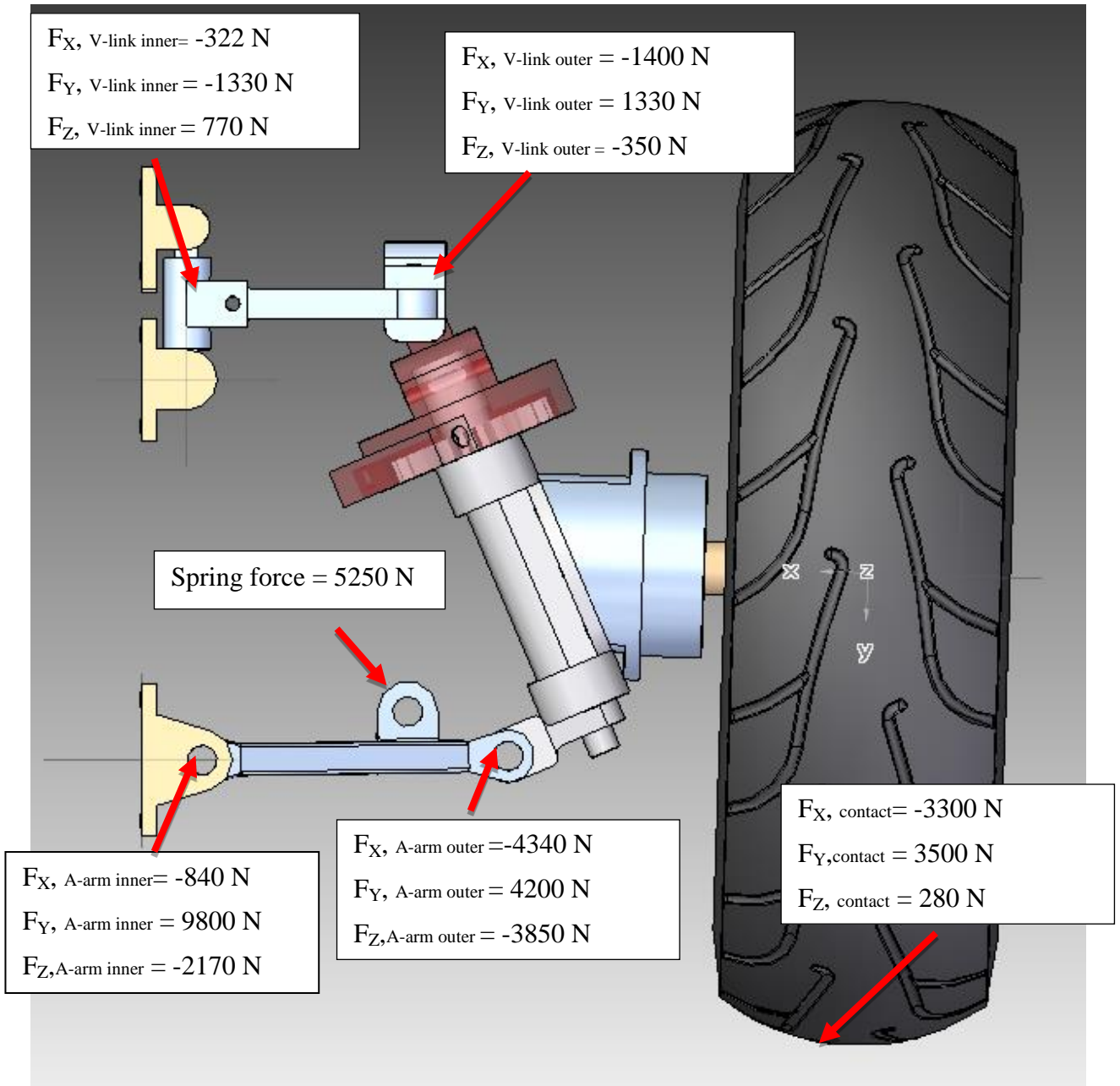


Figure 3.17 Illustration of forces acting in different points of the suspension based on the Adams simulation (with FOS).

4 DETAIL DESIGN

The final CAD models are being designed in parallel with the Adams Car model. The load carrying capabilities of the main components are verified using ANSYS. The steps and materials are discussed here.

The Cad model for each part is modelled using the Solid Edge Cad software. Based on strength requirement, and availability of suitable material, Aluminium alloy 6061 was selected for all the parts.

Aluminum 6061 has the following material strength properties.

Yield Tensile strength	= 2.8 E8 Pa
Ultimate tensile strength	= 3.1 E8 Pa
Density	= 2770 Kg/m ³

The complete assembly of the steering system and its individual part's design are discussed below. For an understanding purpose, the wheel is removed from hub motor in Figure 4.1. The design of supporting elements, such as, lead screw, guide way, worm & wheel are not included in this thesis. The drive unit for steering and camber control system are not show in the picture.

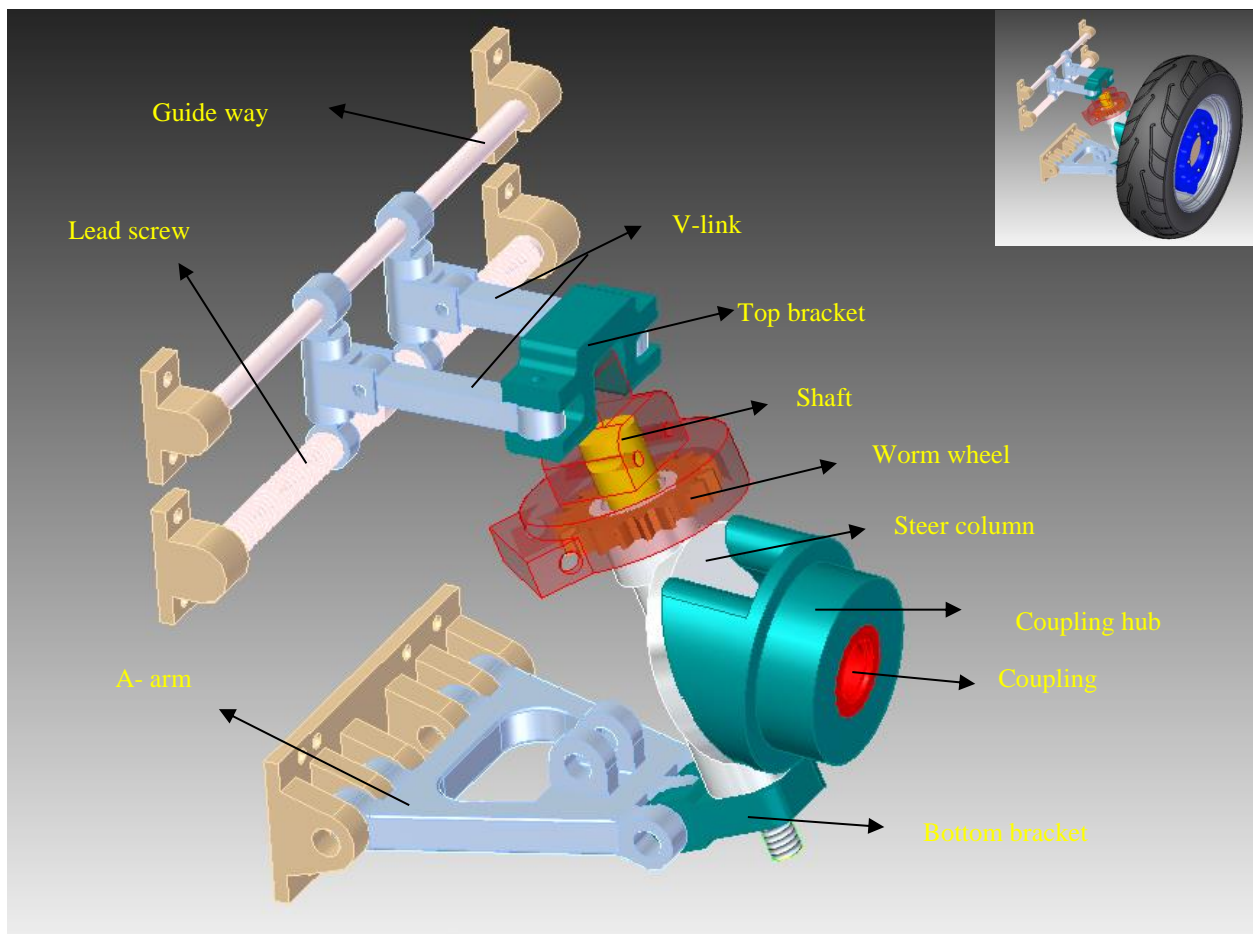


Figure 4.1 Isometric view of steering system

4.1 Hub motor

This car is driven by 4 in-wheel (hub) motors, which has the following specifications (Table 4.1) and characteristics (Figure 4.2).

Table 4.1 Data of selected motor (Heinzmann PRA - 230 48 V DC)

Nominal Power P_N	2.0 kW
Nominal Speed n_N	520 rpm
Nominal Torque M_N	33.0 Nm
Motor Peak torque M_p	150 Nm
Motor Voltage (AC)	33.30V
Motor Current I_N (rms)	42.1 A
Torque-Constant	0.7838 Nm/A

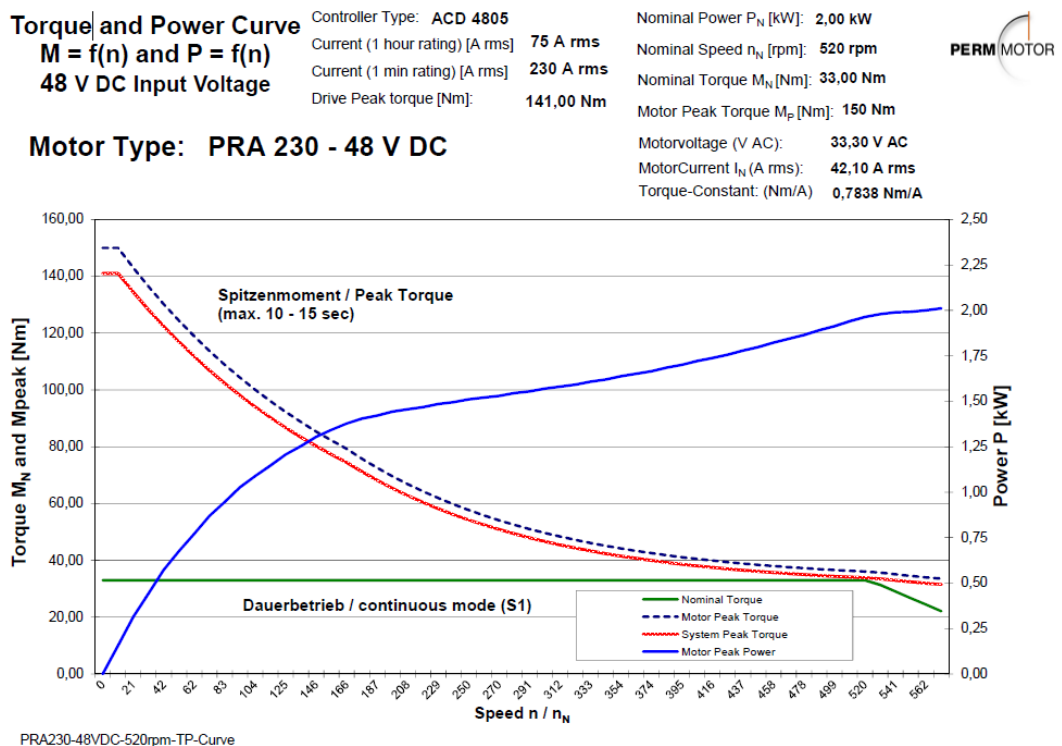


Figure 4.2 Motor speed torque characteristics. [9]

4.2 A-Arm

This is the most strength demanding part in the whole steering system. It was made with a thickness of 25 mm. It connects the frame of the body with the tyre unit. The width of A-arm is over-dimensioned to ensure that it will have a high torsional rigidity during braking or quick acceleration. The resulting stress levels also shows that most of this part is loaded very low with a small high loaded area with a maximum stress of 222 MPa (see figure 4.4).

This is the most strength demanding part in this whole steering system. It is made with the thickness of 25 mm. It connects body frame with the tyre unit and this length is fixed. The width of A-arm is designed bigger so that, it can have maximum torsional rigidity during braking or quick acceleration.

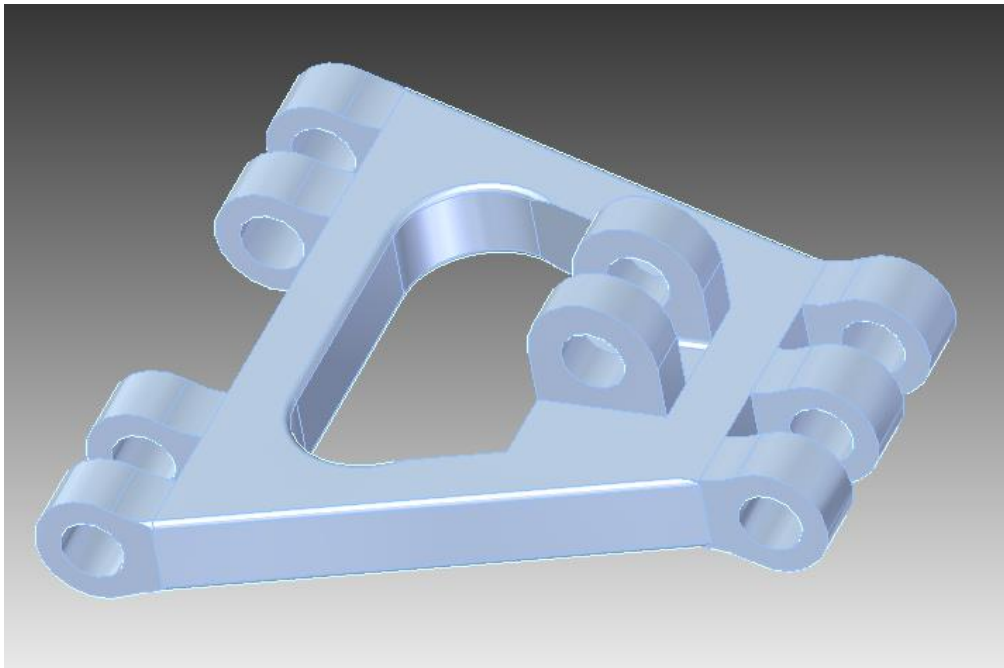


Figure 4.3 CAD model of A-Arm.

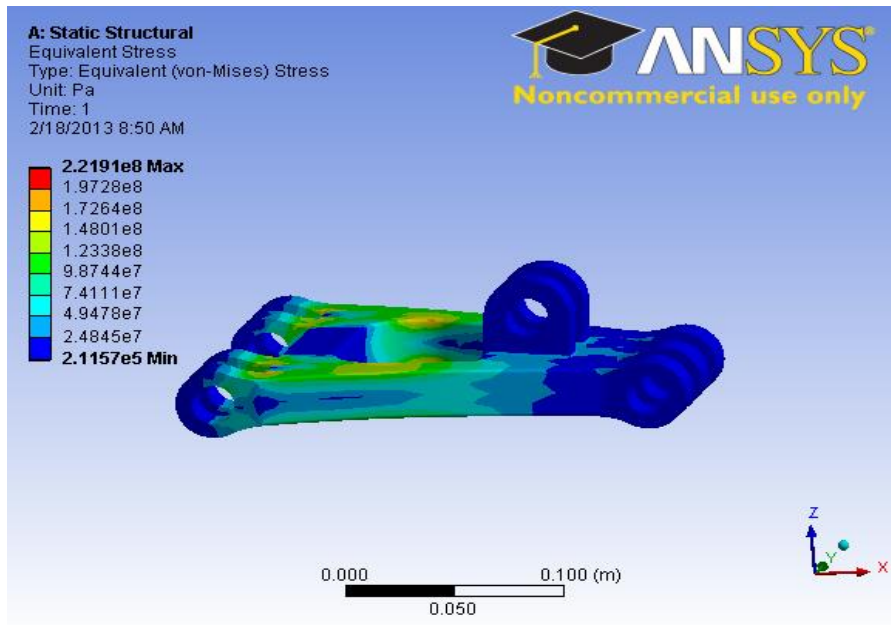


Figure 4.4 ANSYS verification showing stress values.

4.3 Coupling hub

This part actually holds the interference fit motor coupling. This is connected to the steering column using bolts. The planned assembly sequence is as follows; first connect the motor shaft with interference coupling, and then connect this to the coupling hub. Finally it is fitted and bolted to the steering column using the holes shown in Figure 4.5. These holes are perpendicular to the budding plane and not parallel to wheel axis. The load carrying capacity of this part is verified using ANSYS. The result (figure 4.6) shows a maximum stress of 13 MPa which indicates that this part also is over dimensioned.

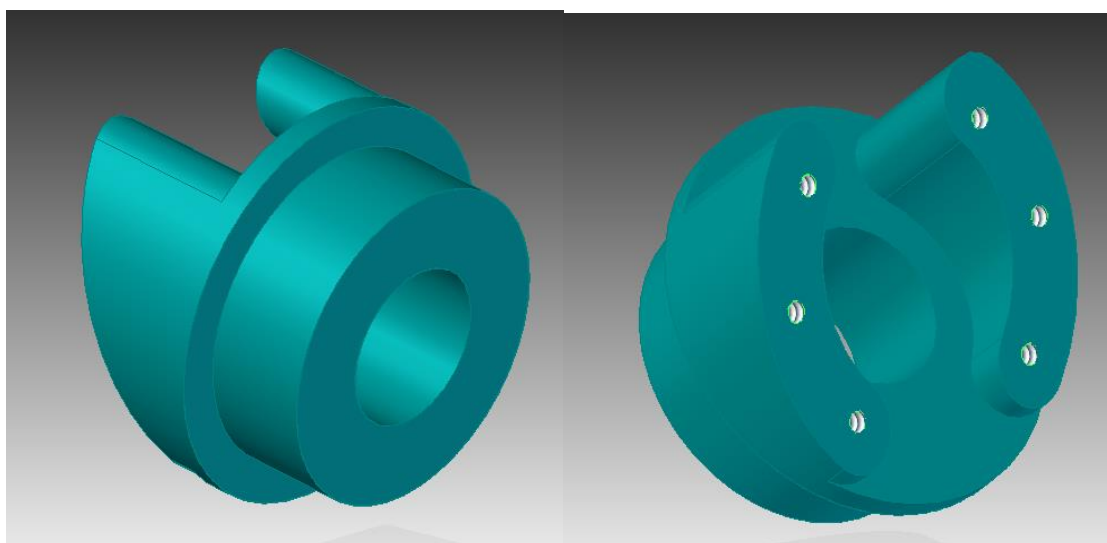


Figure 4.5 CAD Model of Coupling Hub

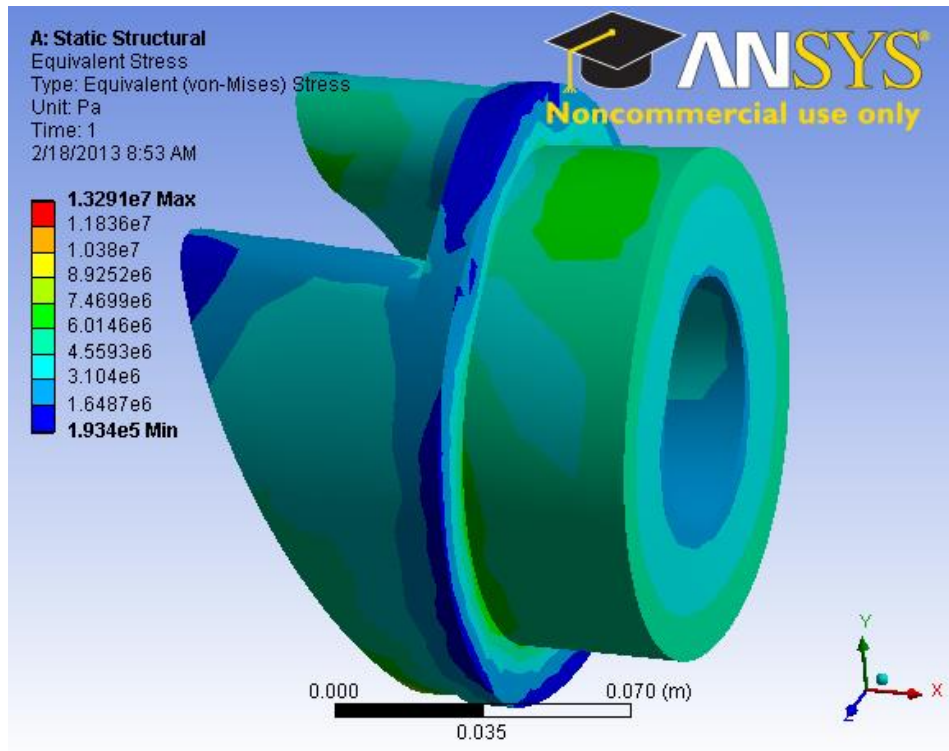


Figure 4.6. ANSYS verification showing stress values.

4.4 Steering column

This is the rotating column that rotates about the fixed shaft which is supported by two taper roller bearings. The bottom end is connected to the A-arm through an adapter bracket. The top end is connected to a variable length V-link through a bracket. This column carries a worm wheel, which is part of a worm gear. This is the actual mechanism for steering the wheel.

The whole column is inclined to 25° from the vertical axis. This reduces the distance between the tyre-road contact point and the point of projection of steering axis, thereby reducing the tyre wear. A fixed shaft that runs through this column is connected to the top bracket with position locking using dowel pins. This does not only locks the shaft's rotation but also keeps the shaft in place axially. The load carrying capacity of this part is verified using ANSYS. The result (Figure 4.8) shows a maximum stress of 1.7 MPa which indicates that this part also is over dimensioned.

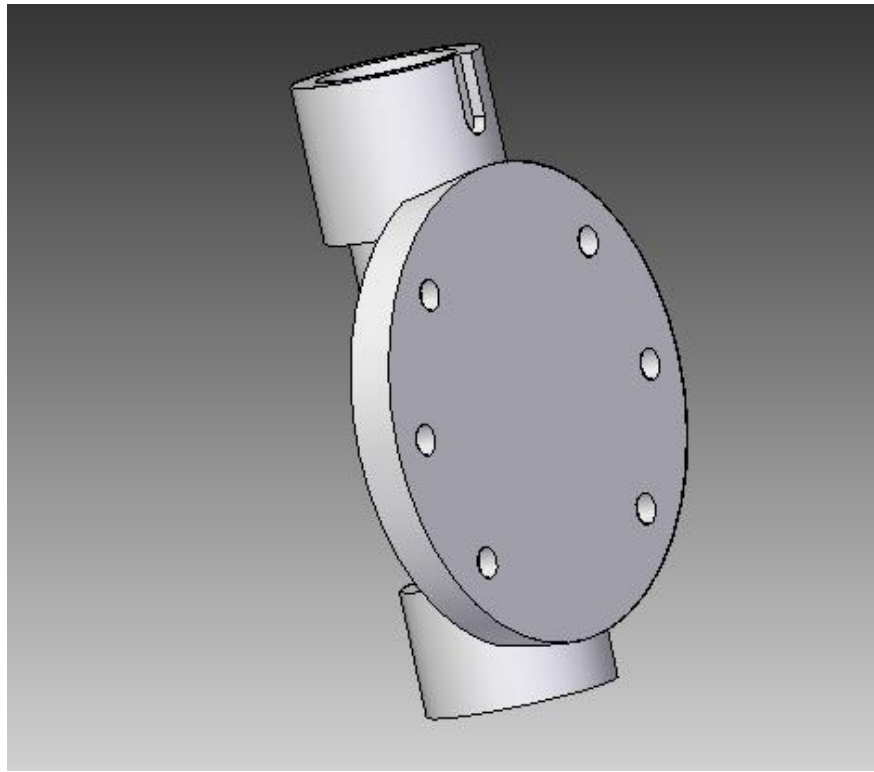


Figure 4.7 CAD model of steering column.

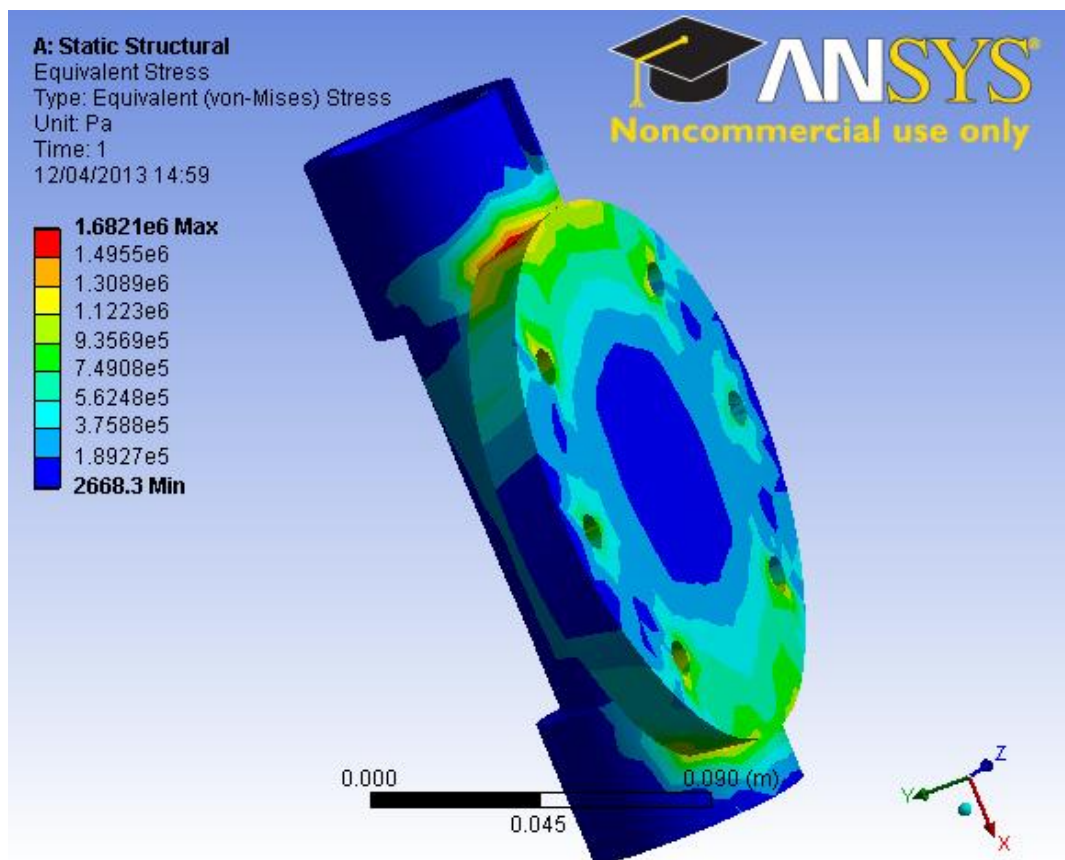


Figure 4.8. ANSYS verification showing stress values.

4.5 Top bracket

This part holds the worm gear which drives the worm wheel. This bracket is attached to the shaft inside the column, and doesn't rotate along the steer column. This bracket is connecting the column to the top pivot.

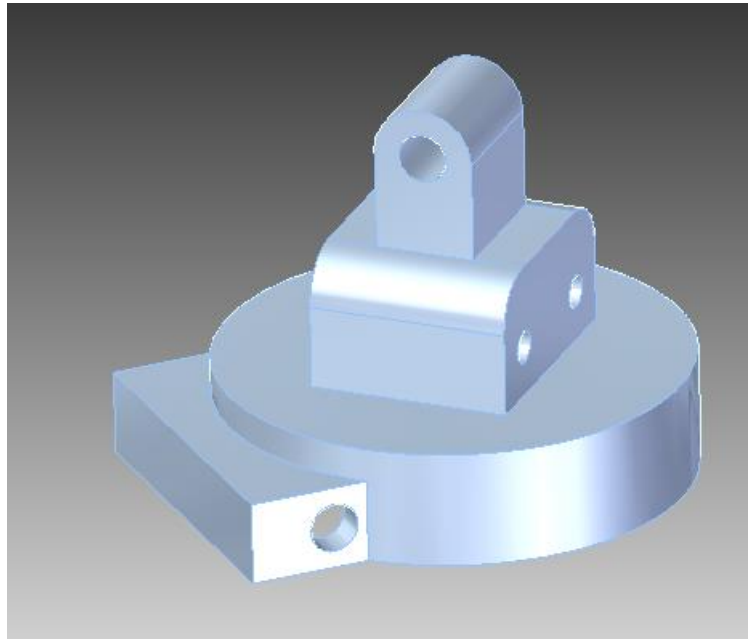


Figure 4.9 CAD model of top bracket

A geometry locking method is used to lock the shaft to this top bracket. The two parallel holes and its corresponding male counterpart will arrest the shaft both in rotation and linear movement in axial direction (see Appendix 2 for further explanation)..

The shaft mating with this top bracket is shown in Figure 4.10.

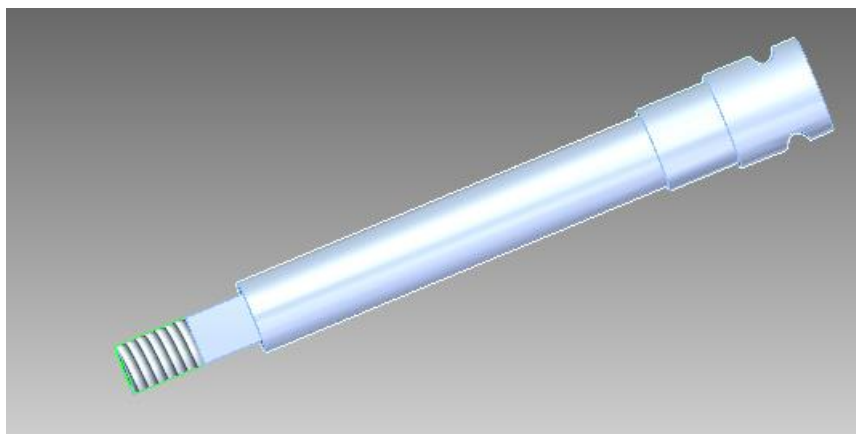


Figure 4.10 CAD model of shaft mating with the top bracket

4.6 Top pivot

This is the part where the two links that forms a “V” at the top end is attached (see figure 4.1). It allows for rotation about two mutually perpendicular axes (see figure 4.11). The resulting stresses in the ANSYS calculations shows that the load on this part is low with a maximum stress of 64 MPa (see figure 4.12).

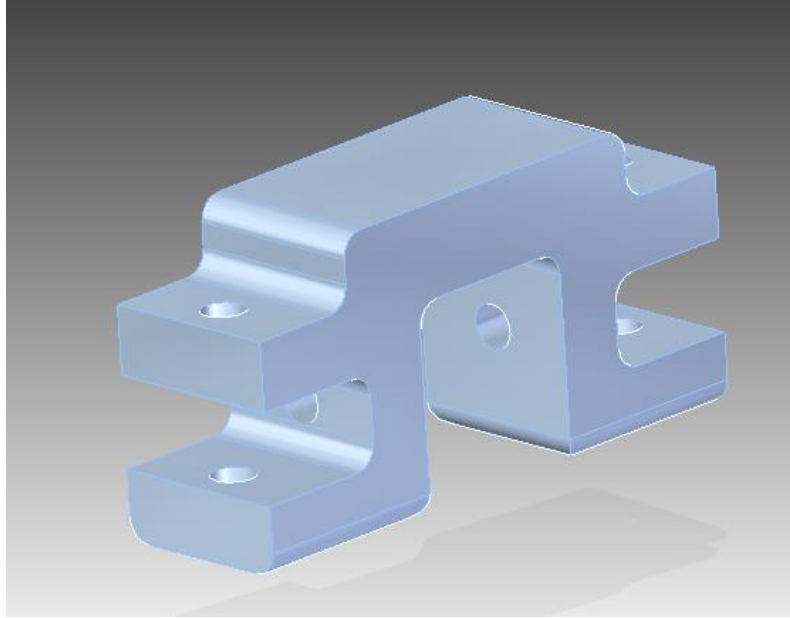


Figure 4.11 CAD model of top pivot

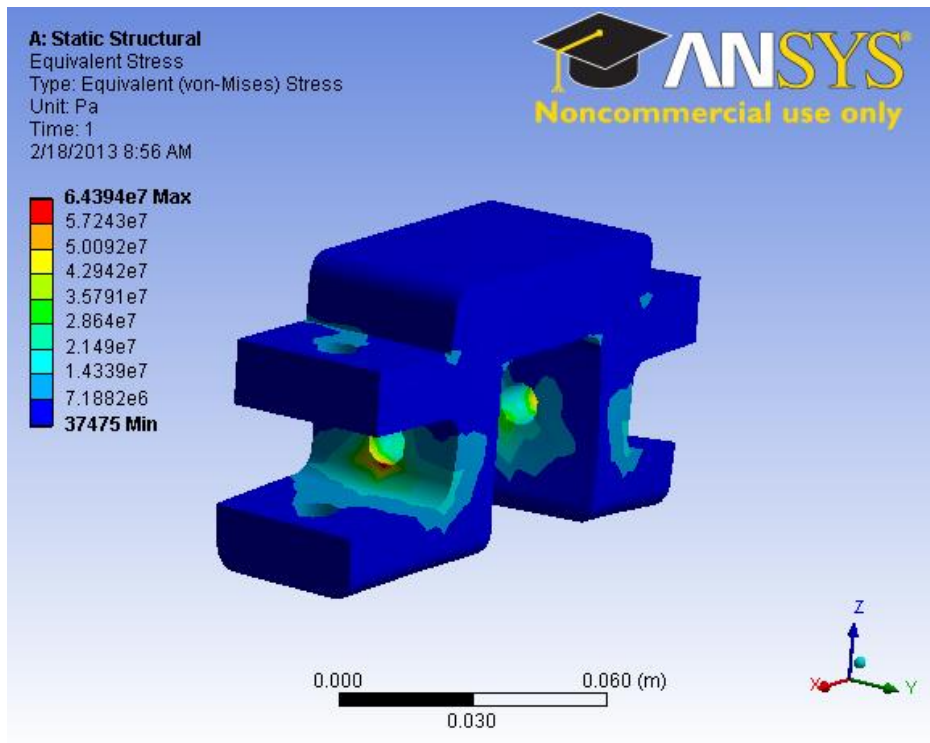


Figure 4.12 ANSYS verification showing stress values.

4.7 V- Link

There are two V-links in this suspension and these are normal straight rigid links (Figure 4.13). These are connected to the top pivot part and the lead screw end (see Figure 4.1). When we turn the lead screw, these two links move apart from each other. This expanding V- angle causes variations in the distance between the top end of steer column and the car body. This is the mechanism that actually changes the steering camber angle. When we control the lead screw rotation we thereby also control the camber angle of the car.

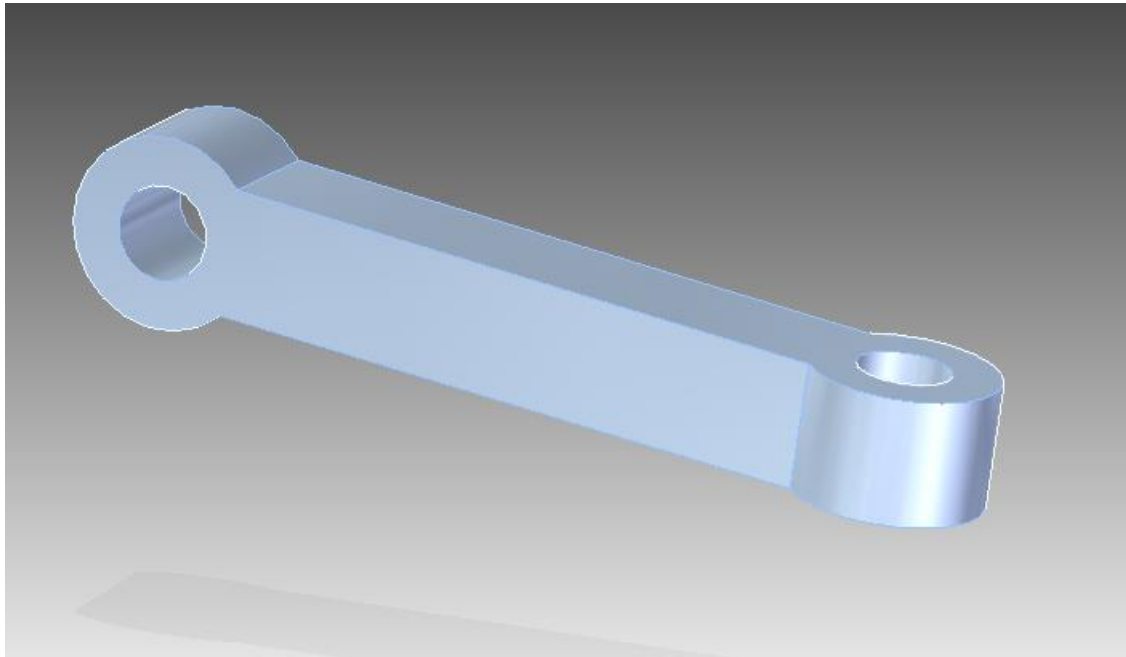


Figure 4.13 CAD model of V- link

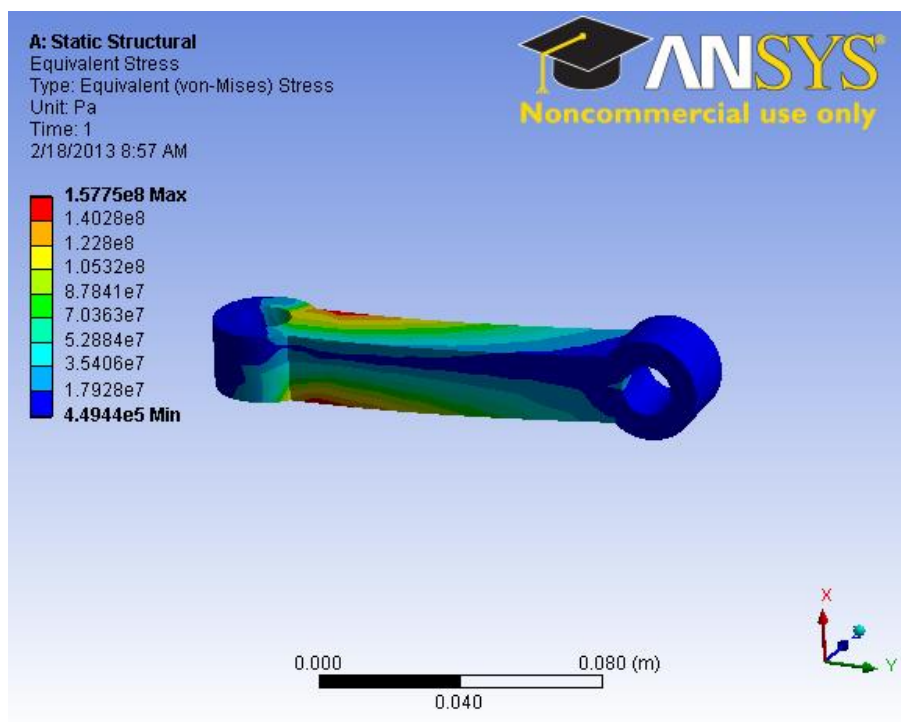


Figure 4.14. ANSYS verification showing stress values.

4.8 Bottom bracket

This bracket is just an adapter that connects fixed shaft inside the steer column with A-arm through a pivot joint. This is not made as integral part of A-arm or the shaft, because of the manufacturing difficulties associated with it.

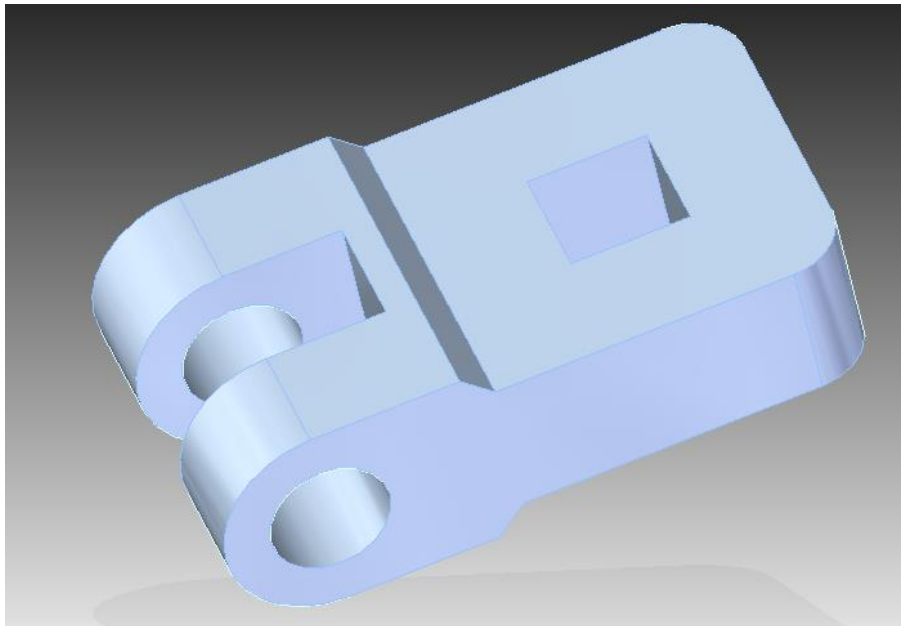


Figure 4.15 CAD model of V- link

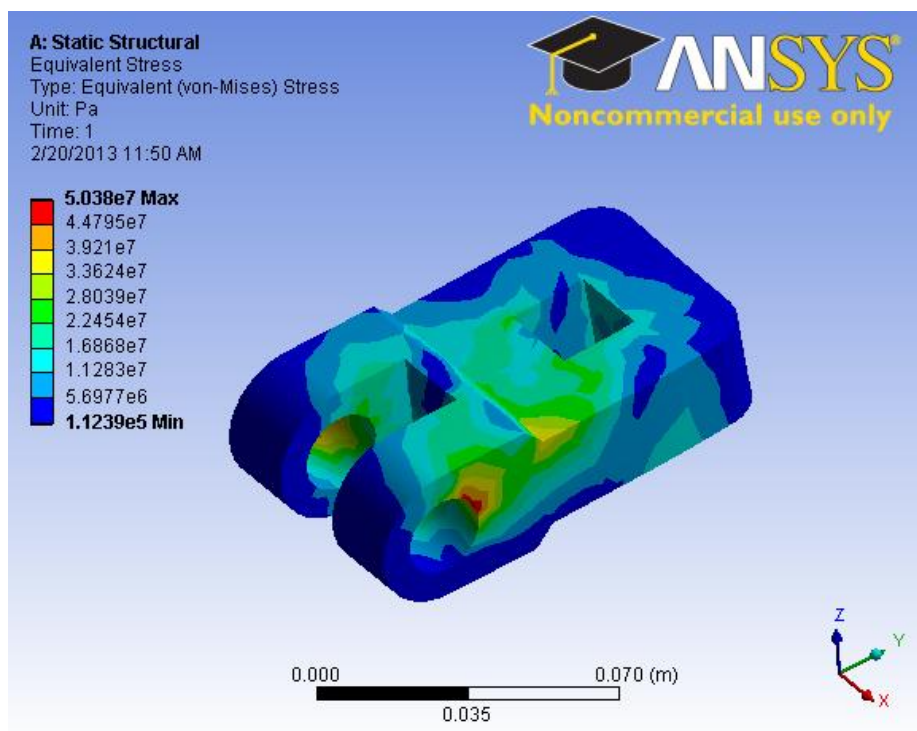


Figure 4.16 ANSYS verification showing stress values.

In all the presented ANSYS verifications, we have found that the maximum stress levels have not exceeded the yield strength of the material. Thus these parts can be manufactured for building the prototype. The assembly drawings and draft sheets of each part were attached in Appendix.

4.9 Range verification of camber angle

The required camber angle range was initially set in the requirement specification is $\pm 10^\circ$. However this range was later changed to -10° to $+5^\circ$.

The resulting suspension was animated in Solid Edge and the camber angle at the extreme positions of the V-links was noted: One extreme position of V-link is when it is kept as close as possible i.e., close to parallel. At this position we get the maximum positive camber angle. This angle was found to be 5° .

The other extreme position is when the V- links are moved as far as possible, i.e. until they reach the end of the lead screw. At this position, we get the maximum negative camber angle which was found to be 12° .

These values satisfy the revised requirement, which was the range -10° to $+5^\circ$. However, the reason for revising the requirements was because this gives better control of the car, e.g. in cornering where always more negative camber is needed.

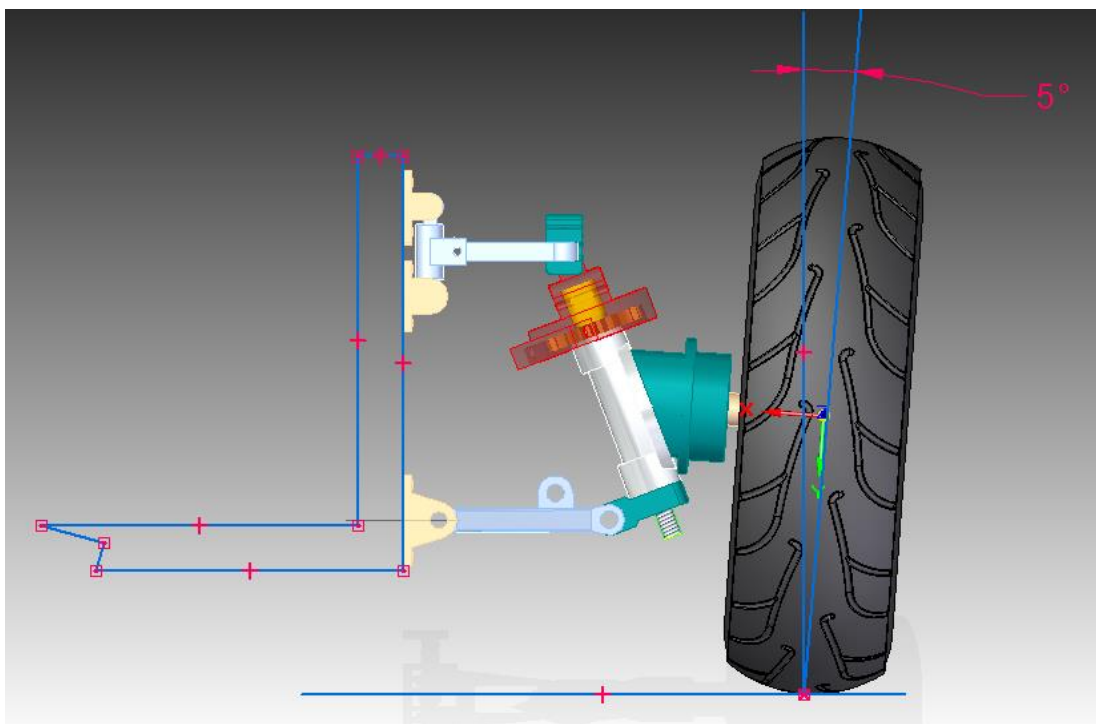


Figure 4.17 CAD model showing maximum positive camber angle.

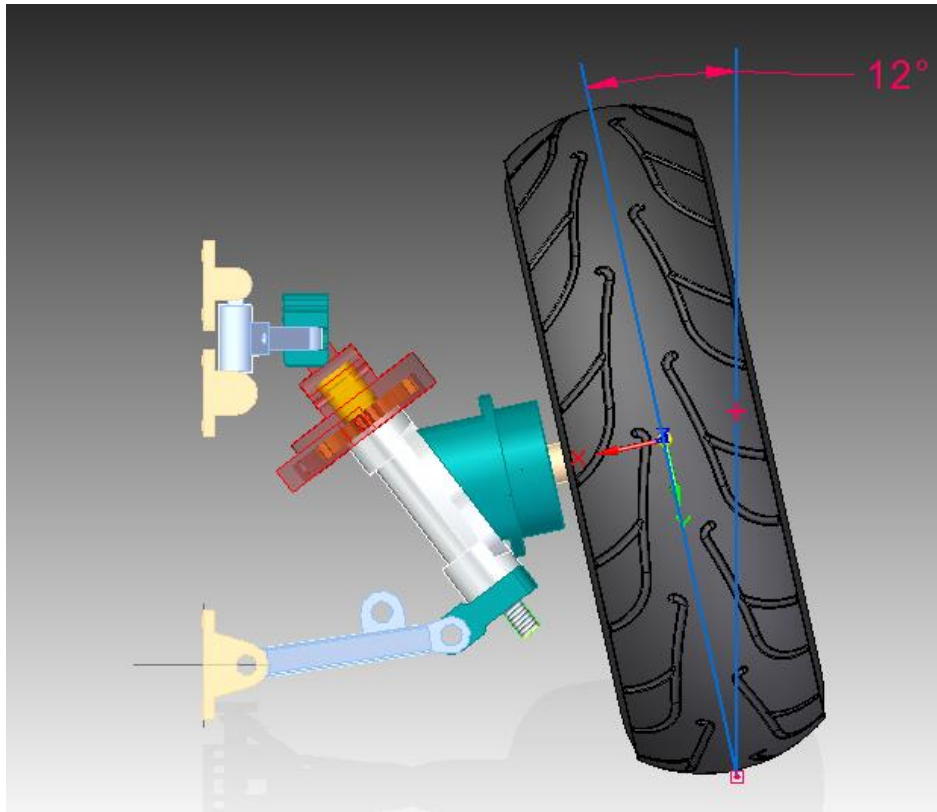


Figure 4.18 CAD model showing maximum negative camber angle

5 DISCUSSION AND CONCLUSIONS

A discussion of the results and the conclusions drawn during the Master of Science thesis are presented in this chapter.

5.1 Discussion

A kinematical model of the selected V-link concept was modelled in Adams Car in order to investigate forces for three main load-cases as well as to check for collisions with the body. This concept was further detailed using the Solid Edge CAD software. Based on some manufacturing constraints, some part models were redefined for better load distribution. Thereafter, these parts were analysed using ANSYS workbench for stress calculations. These analyses showed that all parts were loaded well below its maximum load carrying limits.

The original requirements were set to be -10° to $+10^\circ$ of camber angle variation, but later it was changed to -10° to $+5^\circ$. This change was made because it is always better to have higher negative camber than positive camber in an imbalance situation of a car. The developed solution can set the camber angle between -12° to $+5^\circ$ which satisfies this revised requirement.

Since there were some practical difficulties in manufacturing, some parts were made into two, and assembled together. However, having a single part shall increase strength to weight ratio.

5.2 Conclusions

The following conclusions have been drawn at the end of this thesis:

- A conceptual model of steering system was modelled and its strength was verified.
- For practical difficulty, some parts are modelled based on available manufacturing techniques.
- It is advised to do design optimisation to improve strength to weight ratio.
- In order to obtain the forces due to further test scenarios like crash test, pirouette test, etc., an extension of the current model is recommended.
- The lead screw mechanism could be replaced with any other linear actuators, provide that it has self-locking capabilities without losing much power.

6 RECOMMENDATIONS AND FUTURE WORK

In this chapter, recommendations on more detailed solutions and/or future work in this field are presented.

6.1 Recommendations

Understanding the principles on steering and its control mechanisms is a little tricky and making its components as adjustable is even trickier. This is because the more it becomes adjustable, the more it loses its rigidity. However, a careful investigation of each component and methods to achieve a reliable control could greatly help future drives. There were manufacturing constraints, like casting, welding, in parts like, A-arm, steer column etc.. If we optimize this concept we could get a higher range of adjustability, thus a higher range of camber angle.

6.2 Future work

The following would be a good extension to the work that has already been done:

For this concept, worm and worm wheel selection have not been made. Selecting a suitable worm and wheel set, and proper analysis is needed to implement the final system. There are some minor mechanical elements, like keys, circlips, dowel pin, bearings, pivot pin which have not been selected in the scope of this work. After a complete assembly of the system with all drive line and electronic control units, its performance can be studied, and more design details and concepts can be added.

Instead of lead screw mechanism for varying the V- angle, some linear motor can be used, provided, if it can have self-locking capabilities, without using much of power.

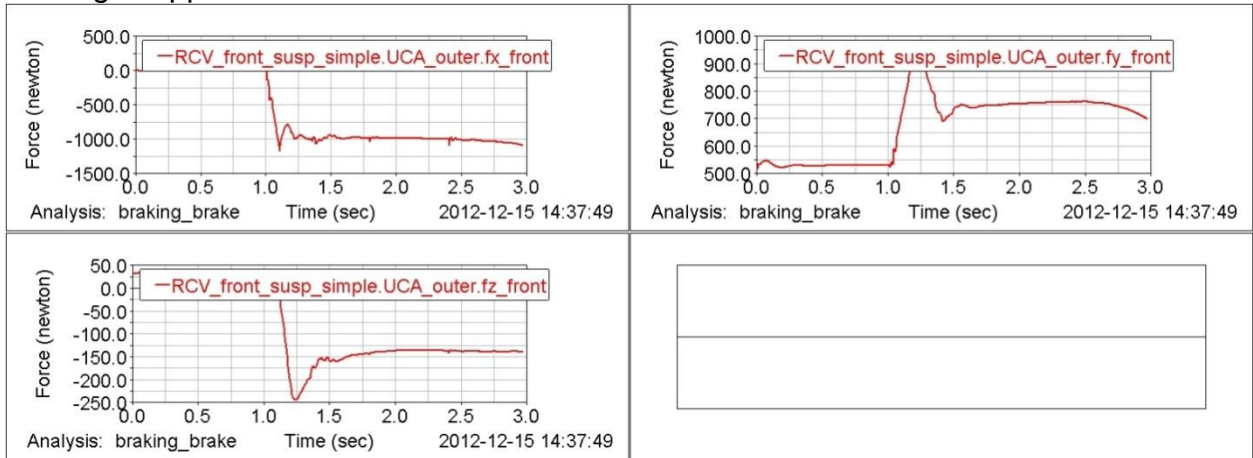
The weight of the system can be reduced without losing its strength, with more detailed study of strength to weight ratio.

7 REFERENCES

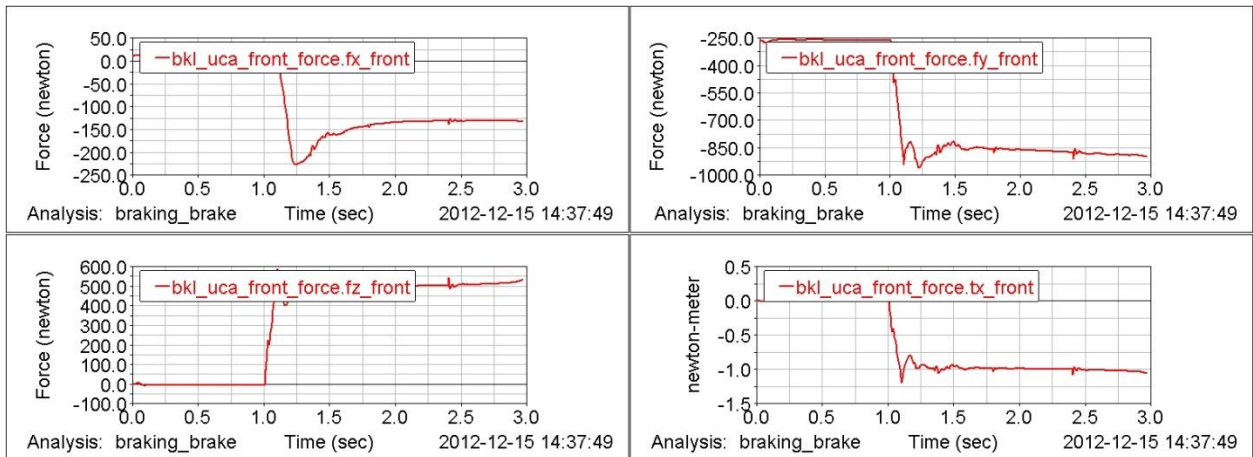
- [1] <http://www.benzworld.org/forums/w126-s-se-sec-sel-sd/1678465-rear-tire-wear-due-negative-camber.html> (Online) Accessed 2013-03-18
- [2] <http://www.wheels-inmotion.co.uk/forum/index.php?showtopic=11082> (Online) Accessed 2013-03-18
- [3] <http://driftjapan.com/blog/car-parts/drift-car-suspension/> (Online) Accessed 2013-03-18
- [4] <http://en.wikipedia.org/wiki/Steering> (Online) Accessed 2013-03-18
- [5] <http://www.howstuffworks.com/steering3.htm> (Online) Accessed 2013-03-18
- [6] http://unionlubeshop.com/power_steering_flush.php (Online) Accessed 2013-03-18
- [7] http://www.carbibles.com/suspension_bible.html (Online) Accessed 2013-03-18
- [8] http://info.hit-karlsruhe.de/Studien-WS08/E_kart_strassenzula/standdertechnik.html (Online) Accessed 2013-03-18
- [9] PERM Motor PRA 230- 48 V DC motor manual.
- [10] http://www.roymech.co.uk/Useful_Tables/ARM/Safety_Factors.html (Online) Accessed 2013-03-18
- [11] “Brake torque characteristics, Web <http://www.ergonomicpartners.com/pdf/Brake-Torque-Application-Data.pdf> (Online) Accessed 2013-03-18
- [12] “Active camber control”, Web <[http://www.fisita2012.com/programme/ programme/F2012-G04-007](http://www.fisita2012.com/programme/programme/F2012-G04-007)>
- [13] “Camber, Caster, Toe”, Web <<http://www.ozebiz.com.au/racetech/theory/align.html>> (Online) Accessed 2013-03-18
- [14] “Suspensions”, Web <http://www.carbibles.com/suspension_bible.html> (Online) Accessed 2013-03-18
- [15] “Steering system”, Web<<http://hdabob.com/Power%20Steering.html>> (Online) Accessed 2013-03-18
- [16] “ADAMS car “, Web, <http://www.me.ua.edu/me364/StudentVersion/Digital_Appendix/car_studentguide_110_071701.pdf>
- [17] V B Bhandari, “Design of Machine Elements”,
- [18] Vehicle Components, “Wheel Suspension and Steering Systems”, KTH – Royal Institute of Technology.
- [19] ANSYS, Computer software, Version. 13.0, <http://www.ansys.com/> (2012). (Online) Accessed 2013-03-18
- [20] Sudhir Kumar Saxena, “Automobile Engineering” Steering systems
- [21] Suresh Verma, “Analysis and design of machine elements”
- [22] Gopinath, K., and Mayuram, Machine Design II, Online Lecture Notes, Indian Institute of Technology, Madras.
- [23] “Pugh Matrix”, Web <http://www.burgehugheswalsh.co.uk/uploaded/documents/Pugh-Matrix-v1.1.pdf> (Online) Accessed 2013-03-18

APPENDIX

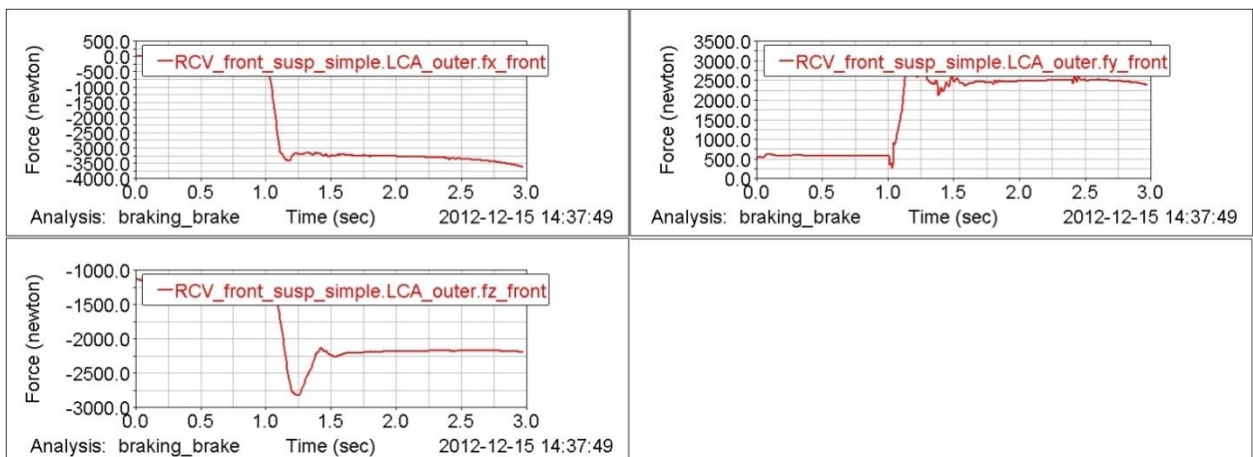
Force plots for the first load case in which the car is run at the speed of 90km/h and full braking is applied.



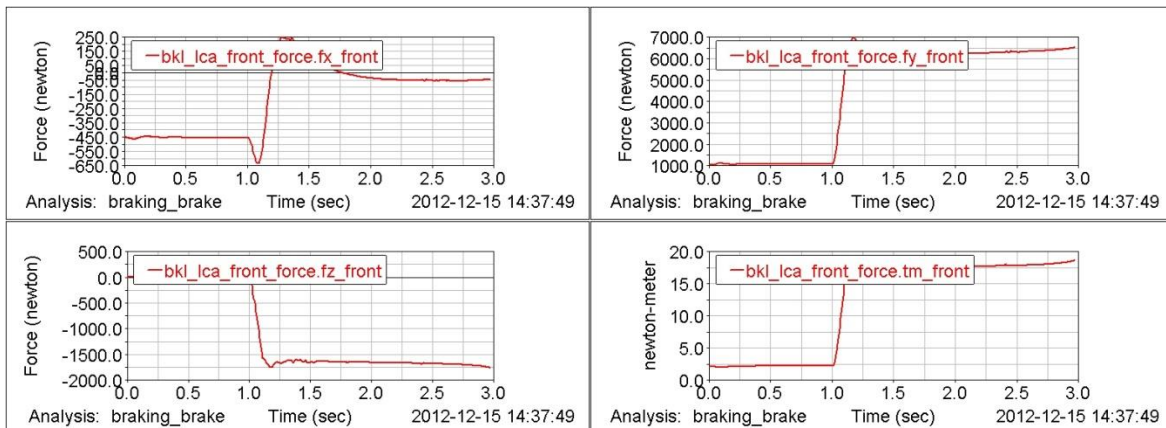
Forces of upper control arm (UCA) outer.



Forces & torque of upper control arm (UCA) inner.

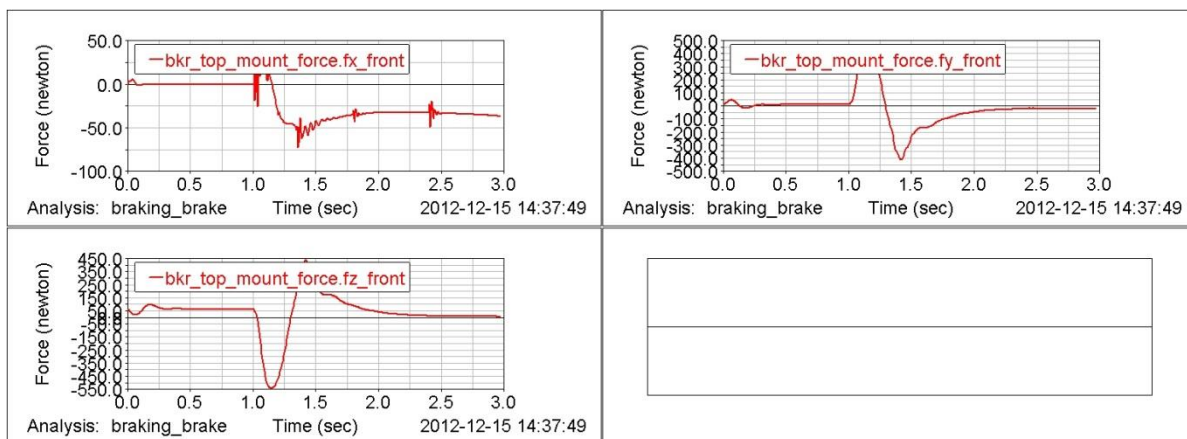


Forces of lower control arm (LCA) outer.

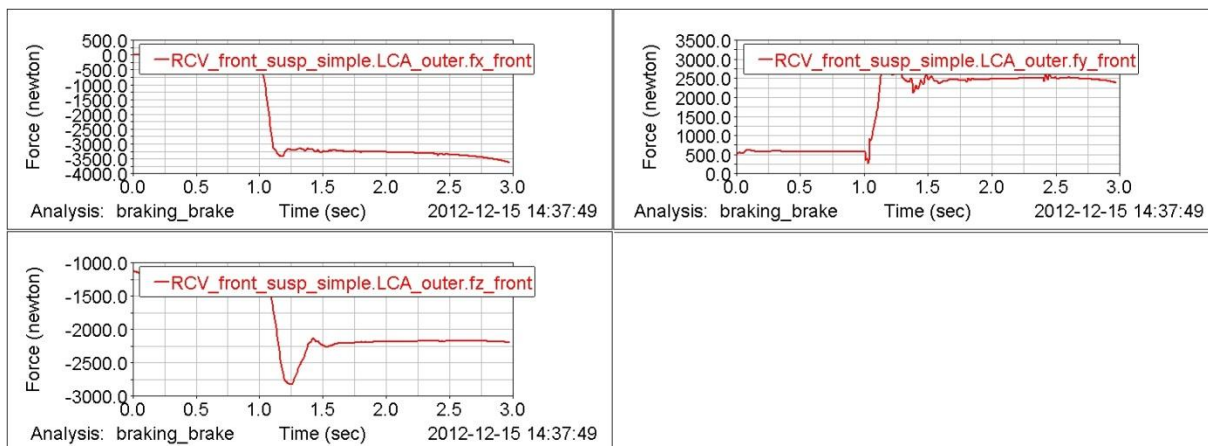


Forces& torque of bracket-left (bkl) lower control arm (LCA).

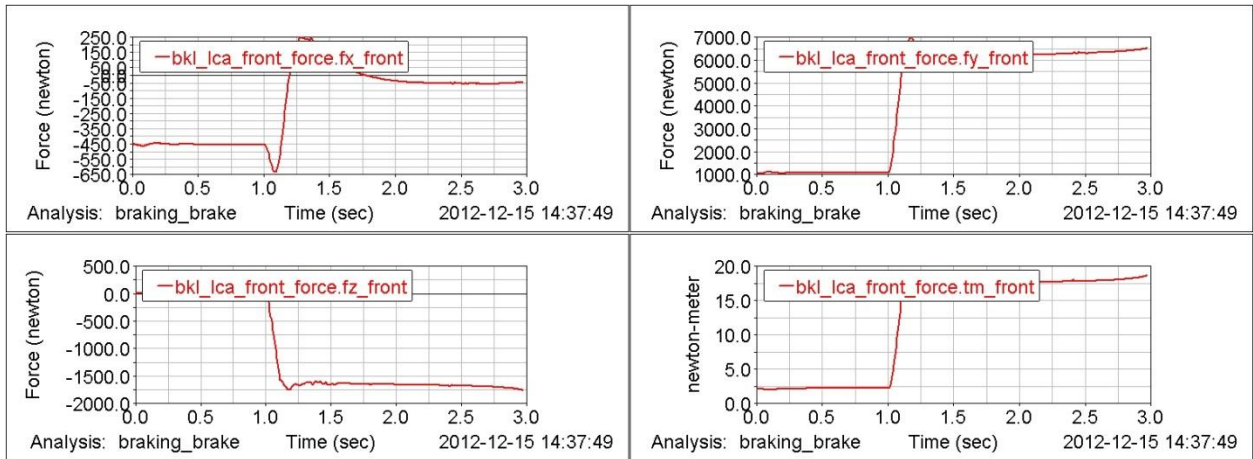
Force plots for the second load case, in which the car is taking a turn of 5m radius.



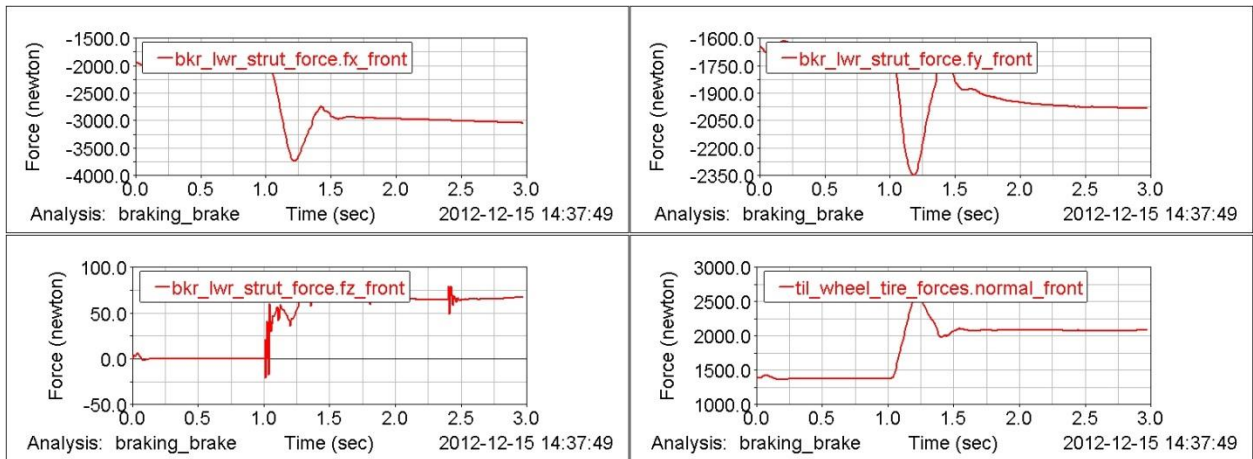
Forces& torque of bracket-right (bkr) lower control arm (LCA).



Forces& torque of suspension.

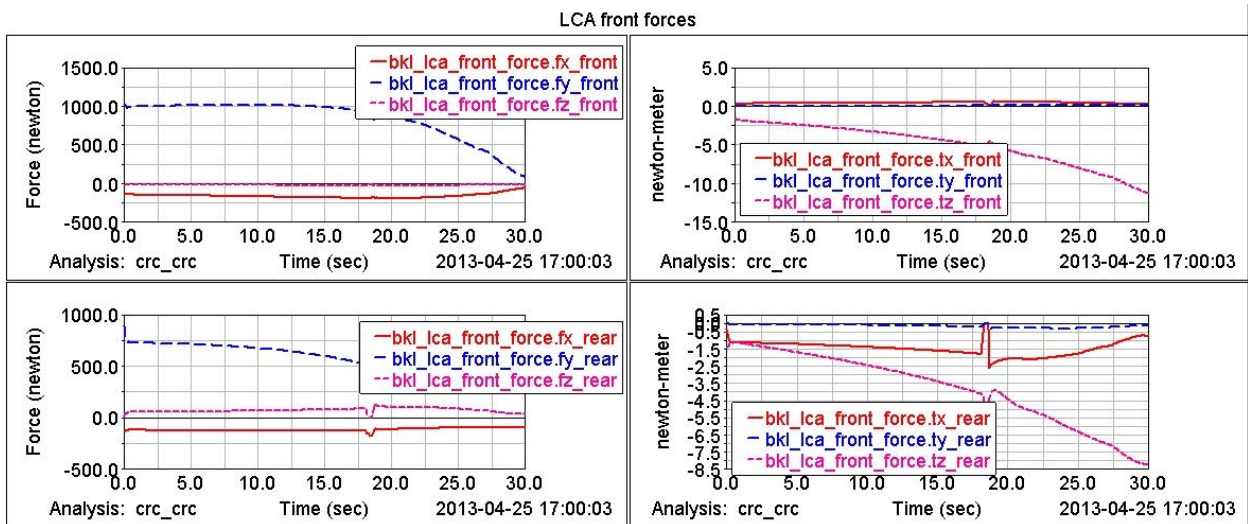


Forces& torque of lower control arm (LCA or A-arm) inner.

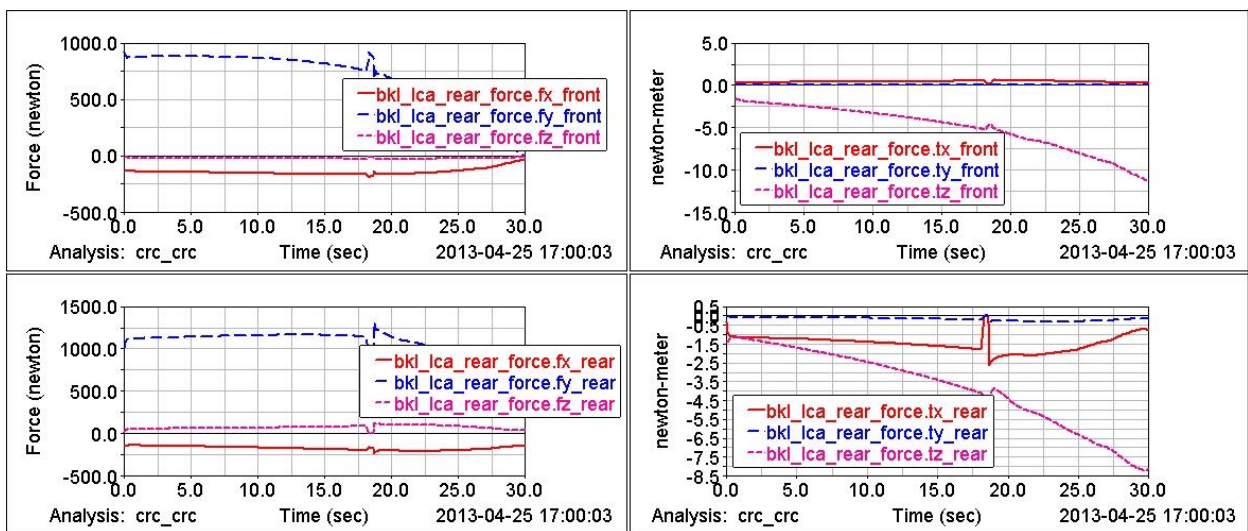


Forces& torque of lower control arm (LCA or A-arm) outer.

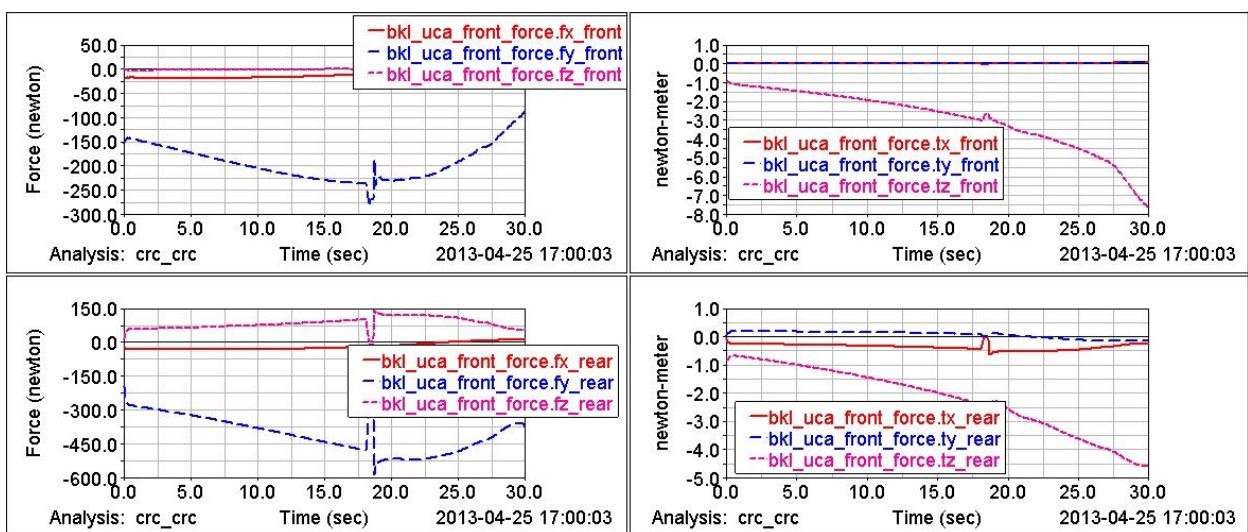
Force plots for the third load case, in which the carencounters a bump of 13cm.



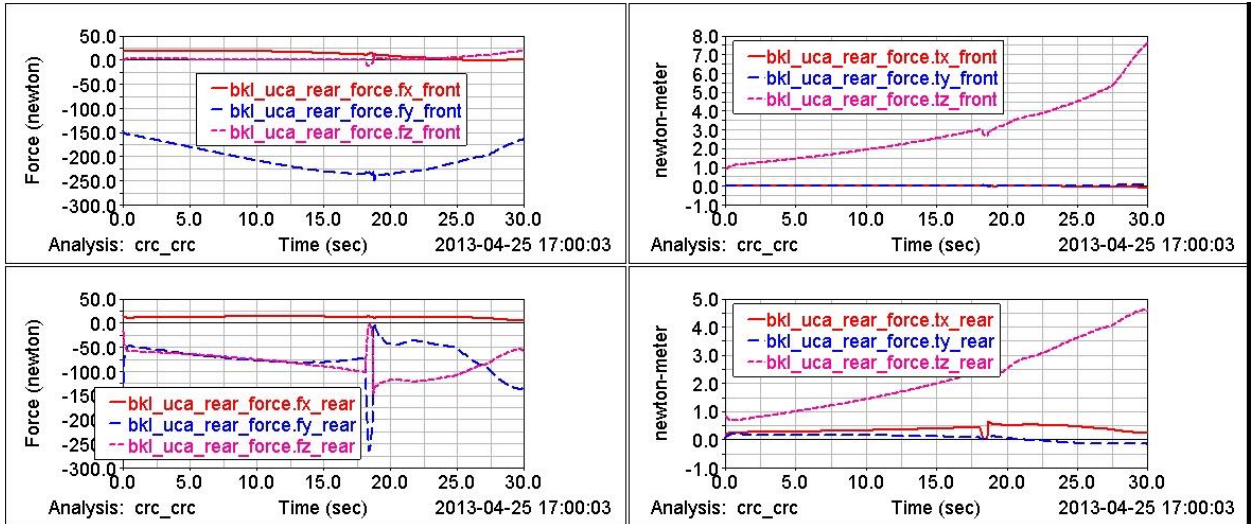
Fores& torque of lower control arm (LCA or A-arm).



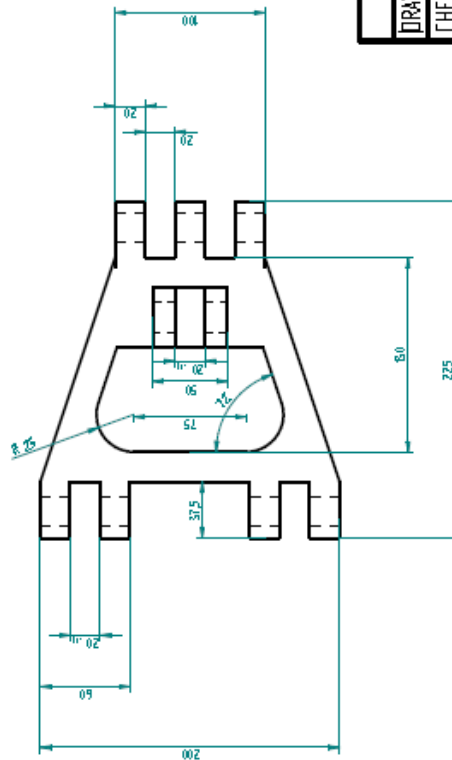
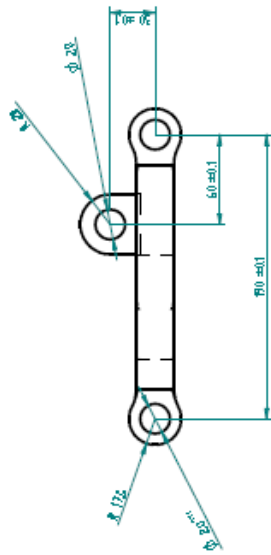
Fores& torque of lower control arm (LCA or A-arm) rear.



Fores& torque of upper control arm (UCA or V-link) front.



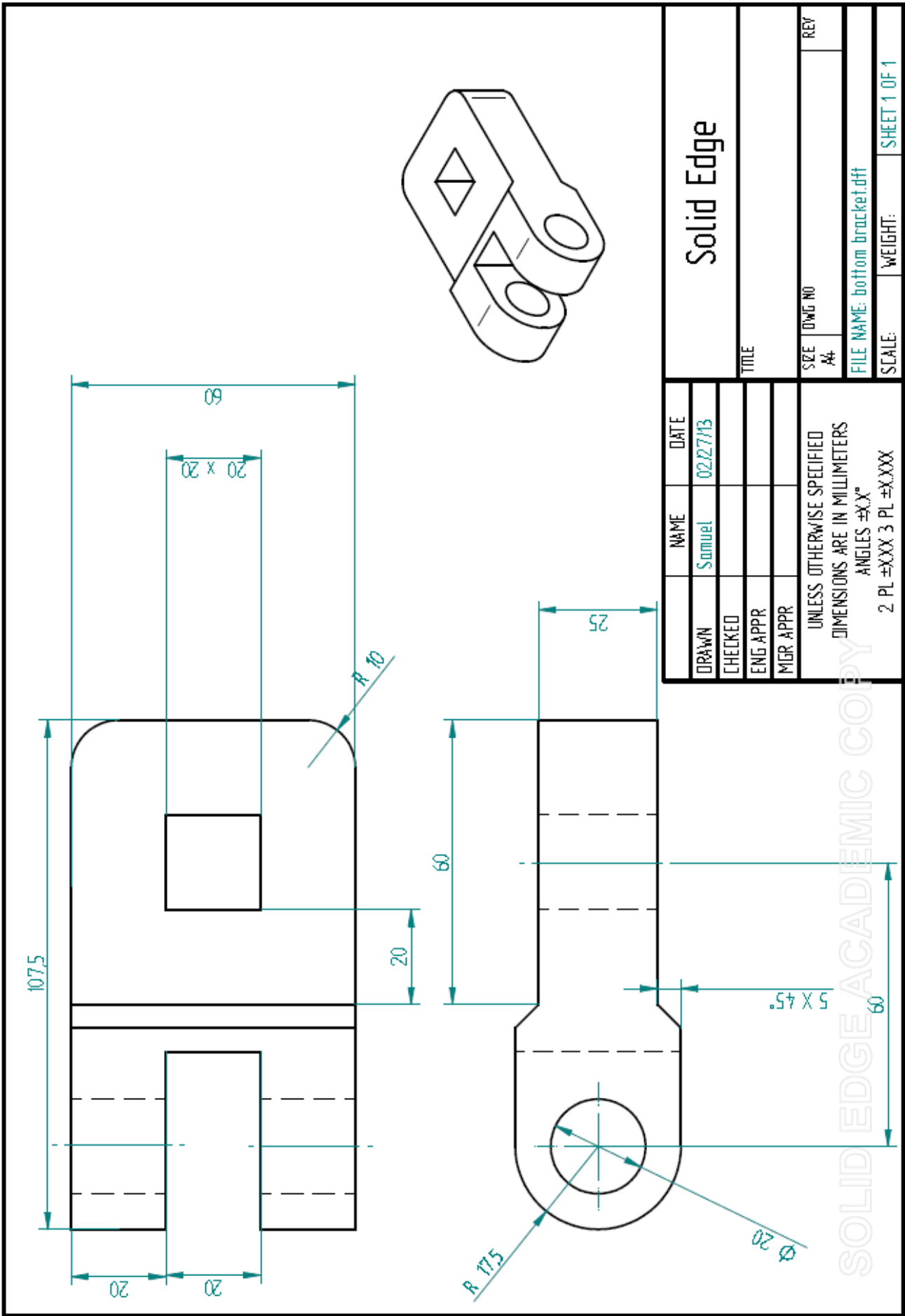
Plot showing forces & torque of upper control arm (UCA or V-link) rear.

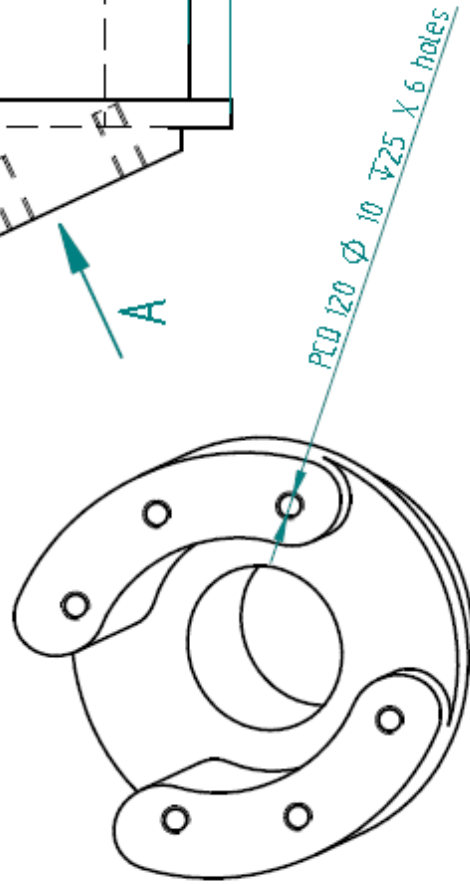
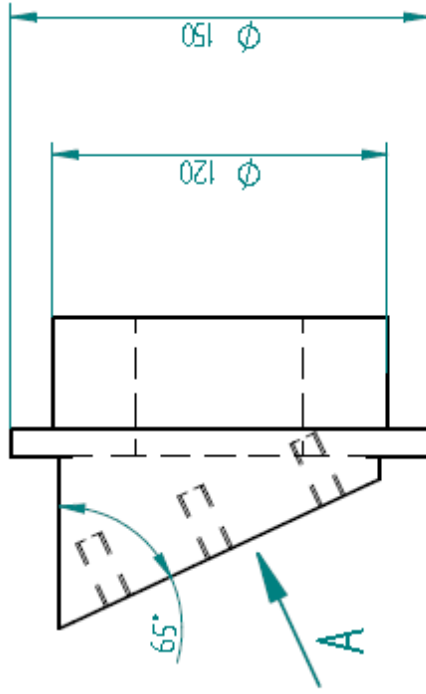
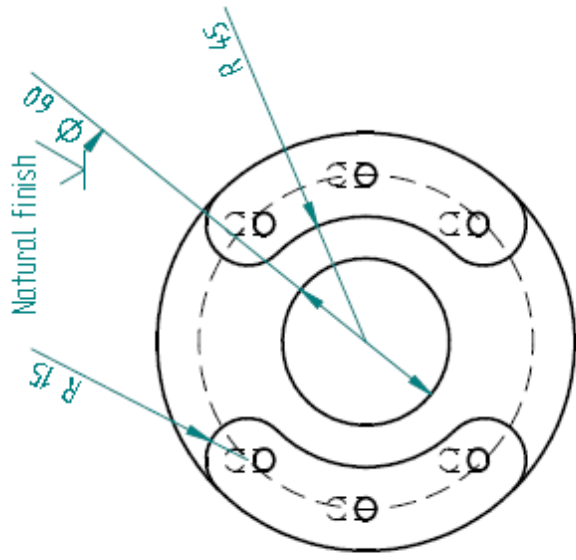


NAME	DATE	Solid Edge	
DRAWN Samuel	02/27/13		
CHECKED		TITLE	
ENG APPR		A- Arm	
MGR APPR		SIZE	DWG NO
		A4	
		FILE NAME: A arm.dft	
		SCALE:	WEIGHT:
		SHEET 1 OF 1	

UNLESS OTHERWISE SPECIFIED
DIMENSIONS ARE IN MILLIMETERS
ANGLES ±XX°
2 PL ±XXX 3 PL ±XXXX

SOLID EDGE ACADEMIC COPY

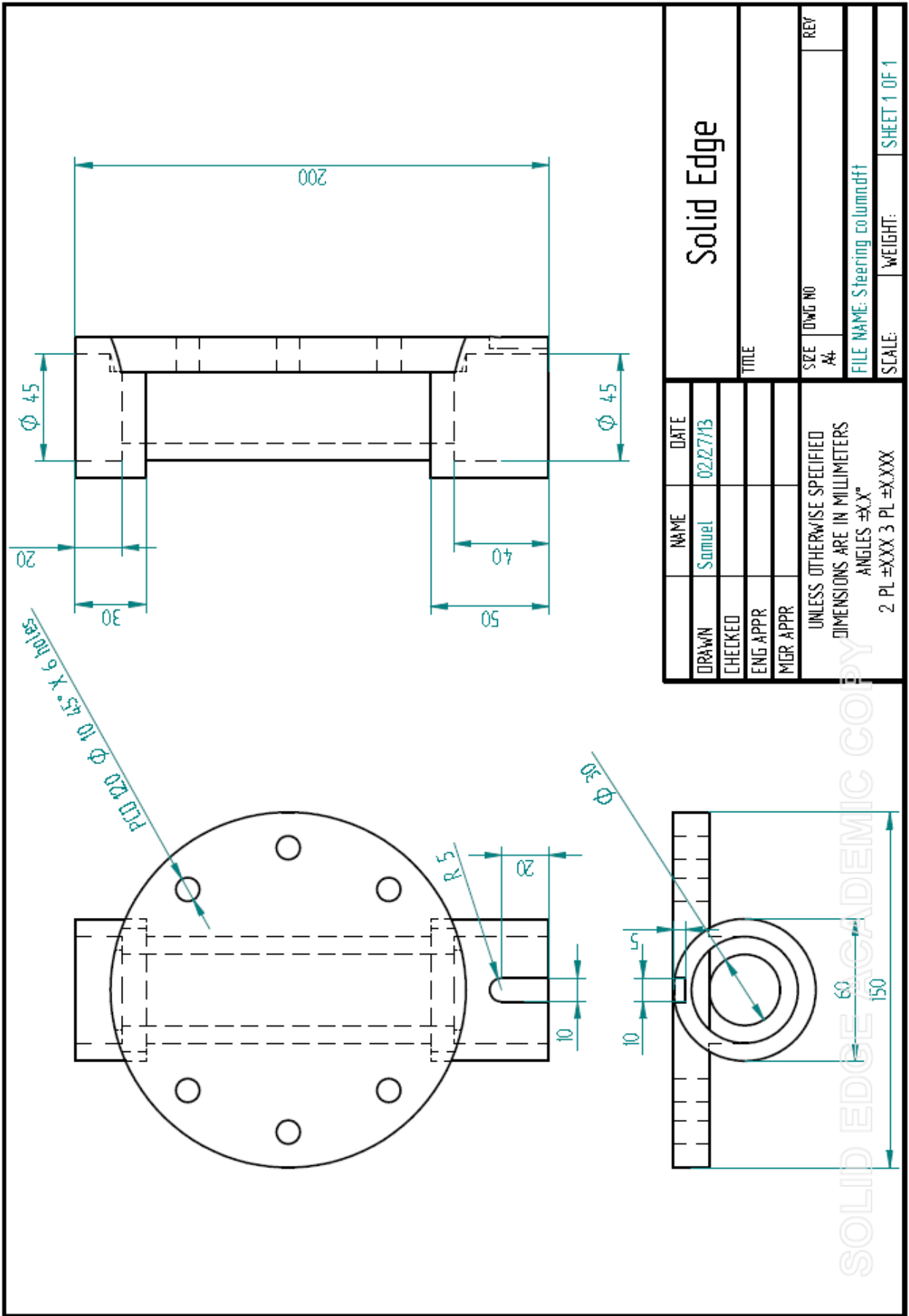


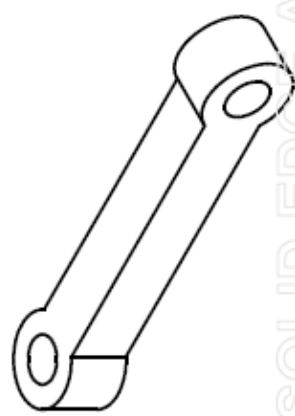
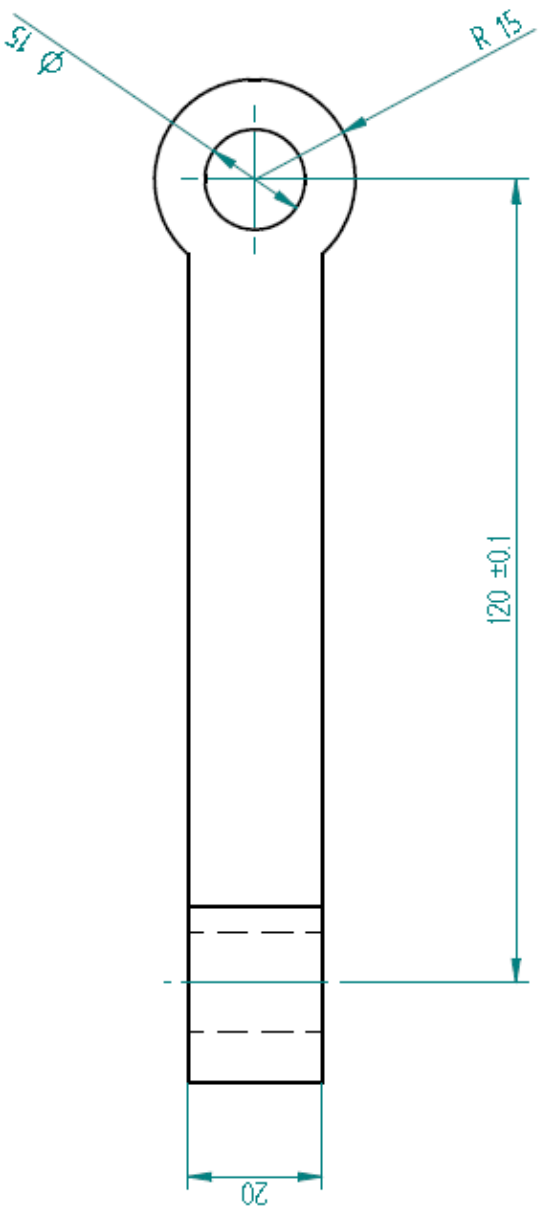


VIEW A

NAME		DATE
DRAWN	Samuel	02/27/13
CHECKED		
ENG APPR		
MGR APPR		
UNLESS OTHERWISE SPECIFIED DIMENSIONS ARE IN MILLIMETERS ANGLES $\pm 0.1^\circ$		
2 PL ± 0.03 3 PL ± 0.04		
TITLE		REV
Solid Edge		
SIZE	DWG NO	REV
A4		
FILE NAME: coupling hubdft		
SCALE:	WEIGHT:	SHEET 1 OF 1

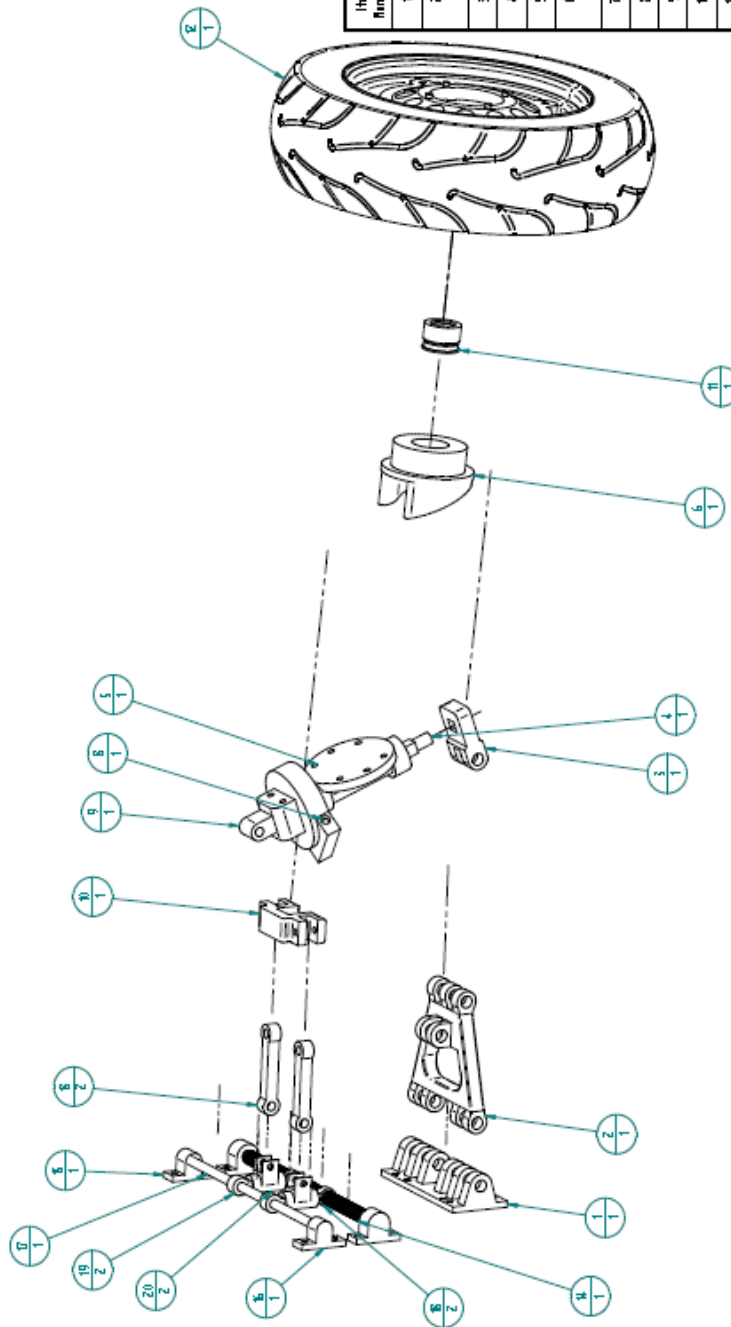
SOLID EDGE ACADEMIC COPY





DRAWN		NAME	DATE	Solid Edge	
CHECKED		Samuel	02/27/13	TITLE	
ENG APPR				SIZE	DWG NO
MGR APPR				A4	REV
UNLESS OTHERWISE SPECIFIED DIMENSIONS ARE IN MILLIMETERS ANGLES ±X°				FILE NAME: V Link.dft	
				SCALE:	WEIGHT:
2 PL ±XXX 3 PL ±X.XXX				SHEET 1 OF 1	

SOLID EDGE ACADEMIC COPY



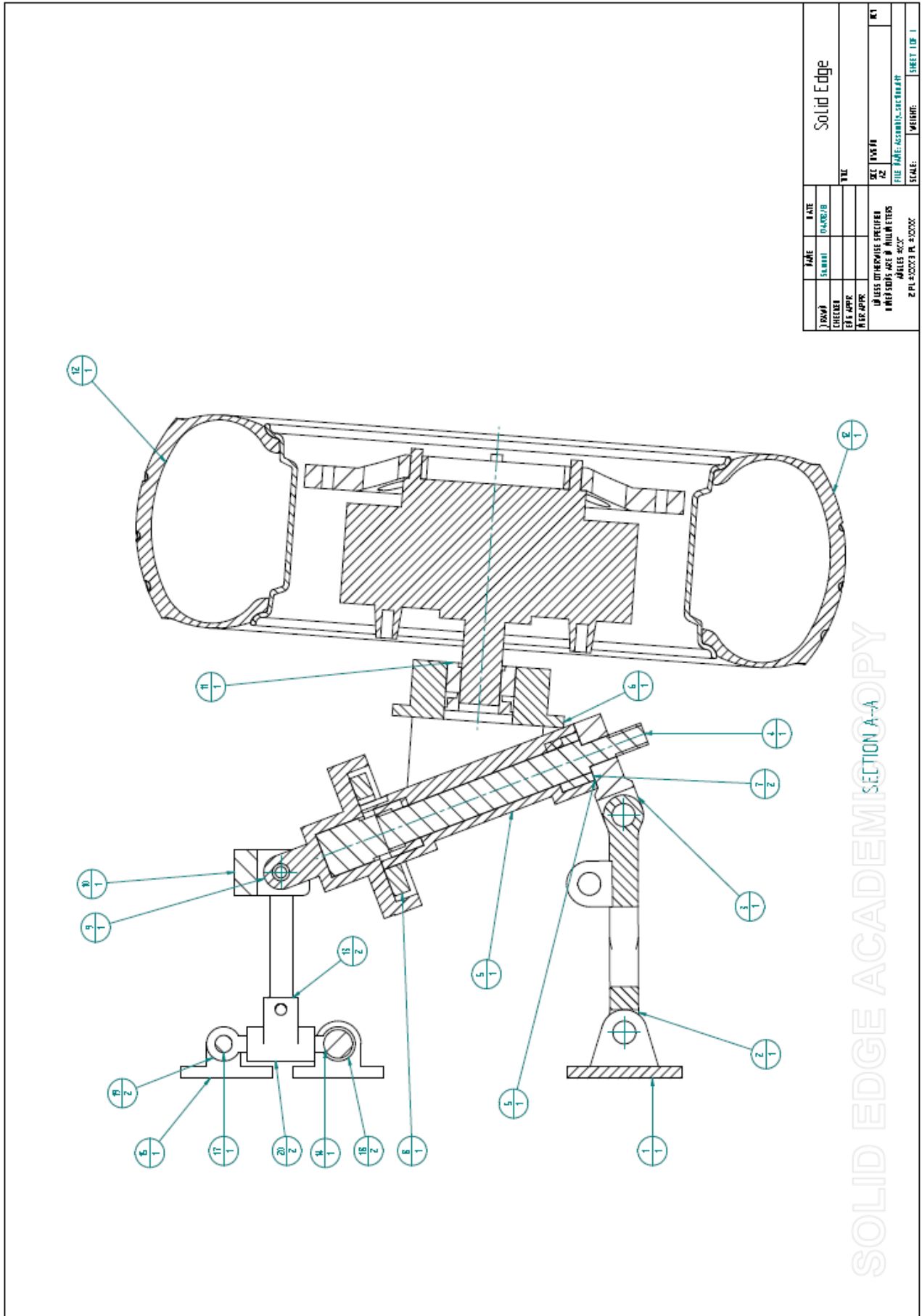
Item Number	Description Number	Title	Material	Quantity
1		Bearing housing		1
2		A - Arm	Aluminum, 6061-T6	1
3		Bottom bracket		1
4		Shaft		1
5		Bearing column		1
6		Coupling hub	Aluminum, 8080	1
7		Taper roller bearing		1
8		Worm Wheel		1
9		Top Bracket		1
10		Top Plate		1
11		Interference coupling		1
12		Motor and Wheel assembly		1
13		Y - Link		2
14		Lead Screw		1
15		Bearing Flange		1
16		Bearing mount		1
17		Guide vee		1
18		Slider screw		2
19		Slider Guide		2
20		Slider plate		2

DATE	DATE	DATE	DATE
DESIGN	DESIGN	DESIGN	DESIGN
ENGINEER	ENGINEER	ENGINEER	ENGINEER
CHK APPR	CHK APPR	CHK APPR	CHK APPR
MR APPR	MR APPR	MR APPR	MR APPR

Solid Edge

SEC 000710	REV
02	
FILE NAME: ASSEMBLY.PRT	
SCALE:	WEIGHT:
SHEET 1 OF 1	

SOLID EDGE ACADEMIC COPY



SOLID EDGE ACADEMIC SECTION A-A

Item Number	Document Number	Title	Material	Quantity
1		Bearing Housing		1
2		A - Arm	Aluminum, 6061-T6	1
3		Bottom bracket	Aluminum, 6061-T6	1
4		Shaft	Aluminum, 6061-T6	1
5		Steering column	Aluminum, 6061-T6	1
6		Coupling hub	Aluminum, 6061-T6	1
7		Taper roller bearing		2
8		Worm Wheel	Bronze	1
9		Top Bracket	Aluminum, 6061-T6	1
10		Top Pivot	Aluminum, 6061-T6	1
11		Interference Coupling	Steel	1
12		Motor and Wheel assembly		1
13		Y - Link	Aluminum, 6061-T6	2
14		Lead Screw		1
15		Bearing Mount		1
16		Bearing mount		1
17		Guide way		1
18		Slider screw		2
19		Slider Guide		2
20		Slider pivot		2